NAVAL POSTGRADUATE SCHOOL

MONTEREY, CALIFORNIA

THESIS

CONSTRUCTION AND TESTING OF COMPACT LOW-NOISE HYDROPHONES WITH EXTENDED FREQUENCY RESPONSE

by

Konstantinos Bakas

June 2004

Thesis Advisor:	Thomas J. Hofler
Co-Advisor:	Bruce Denardo

Approved for public release; distribution is unlimited

THIS PAGE INTENTIONALLY LEFT BLANK

REPORT DOCUMENTATION PAGE			Form Approved OMB No. 0704-0188
Public reporting burden for this collection of information is estimated to average 1 hour per response, including the time for reviewing instruction, searching existing data sources, gathering and maintaining the data needed, and completing and reviewing the collection of information. Send comments regarding this burden estimate or any other aspect of this collection of information, including suggestions for reducing this burden, to Washington headquarters Services, Directorate for Information Operations and Reports, 1215 Jefferson Davis Highway, Suite 1204, Arlington, VA 22202-4302, and to the Office of Management and Budget, Paperwork Reduction Project (0704-0188) Washington DC 20503.			
1. AGENCY USE ONLY ***(Leave blank)***	**2. REPORT DATE** June 2004	**3. REPORT TYPE AND DATES COVERED** Master's Thesis	
4. TITLE AND SUBTITLE: Construction and Testing of Low Noise Hydrophones			**5. FUNDING NUMBERS**
6. AUTHOR (S) Konstantinos Bakas			
7. PERFORMING ORGANIZATION NAME (S) AND ADDRESS(ES) Naval Postgraduate School Monterey, CA 93943-5000			**8. PERFORMING ORGANIZATION REPORT NUMBER**
9. SPONSORING /MONITORING AGENCY NAME(S) AND ADDRESS(ES) N/A			**10. SPONSORING/MONITORING AGENCY REPORT NUMBER**
11. SUPPLEMENTARY NOTES The views expressed in this thesis are those of the author and do not reflect the official policy or position of the Department of Defense or the U.S. Government.			
12a. DISTRIBUTION / AVAILABILITY STATEMENT Approved for public release; distribution is unlimited.			**12b. DISTRIBUTION CODE**

13. ABSTRACT (maximum 200 words)

A simple low-noise hydrophone design with internal preamplifier is presented. This design is similar to published designs and is a variation of the design developed in the NPS thesis by Miguel Alvarado [2003], except that several improvement features are included. These include a simplification of the structure and its modes of vibration, a large reduction in package diameter and the effect its acoustic diffraction has on the sensitivity, and an extended upper frequency response of 42 kHz resulting from the simplified structure and reduced diameter. Furthermore, the modified geometry along with its orientation in the water should produce a very omni-directional response in the horizontal plane at the higher frequencies. Finally, an new feedback preamplifier design developed by Hofler and Alvarado was discovered to have some subtle but serious performance problems. These problems were resolved in this research and the resulting preamplifier performance was tested and documented herein.

14. SUBJECT TERMS Hydrophone, Sound Receiver, Transducer, Low Noise Preamplifier			**15. NUMBER OF PAGES** 77
			16. PRICE CODE
17. SECURITY CLASSIFICATION OF REPORT Unclassified	**18. SECURITY CLASSIFICATION OF THIS PAGE** Unclassified	**19. SECURITY CLASSIFICATION OF ABSTRACT** Unclassified	**20. LIMITATION OF ABSTRACT** UL

NSN 7540-01-280-5500 Standard Form 298 (Rev. 2-89)
Prescribed by ANSI Std. 239-18

THIS PAGE INTENTIONALLY LEFT BLANK

Approved for public release; distribution is unlimited

CONSTRUCTION AND TESTING OF LOW-NOISE HYDROPHONES

Konstantinos Bakas
Lieutenant, Hellenic Navy
B.S., Hellenic Naval Academy, 1994

Submitted in partial fulfillment of the
requirements for the degree of

MASTER OF SCIENCE IN APPLIED PHYSICS

from the

NAVAL POSTGRADUATE SCHOOL
June 2004

Author: Konstantinos Bakas

Approved by: Thomas J. Hofler
Thesis Advisor

Bruce Denardo
Second Reader

James H. Luscombe
Chairman, Department of Physics

THIS PAGE INTENTIONALLY LEFT BLANK

ABSTRACT

A simple low-noise hydrophone design with internal preamplifier is presented. This design is similar to published designs and is a variation of the design developed in the NPS thesis by Miguel Alvarado [2003], except that several improvement features are included. These include a simplification of the structure and its modes of vibration, a large reduction in package diameter and the effect its acoustic diffraction has on the sensitivity, and an extended upper frequency response of 42 kHz resulting from the simplified structure and reduced diameter. Furthermore, the modified geometry along with its orientation in the water should produce a very omni-directional response in the horizontal plane at the higher frequencies. Finally, an new feedback preamplifier design developed by Hofler and Alvarado was discovered to have some subtle but serious performance problems. These problems were resolved in this research and the resulting preamplifier performance was tested and documented herein.

THIS PAGE INTENTIONALLY LEFT BLANK

TABLE OF CONTENTS

THIS PAGE INTENTIONALLY LEFT BLANK

LIST OF FIGURES

THIS PAGE INTENTIONALLY LEFT BLANK

LIST OF TABLES

THIS PAGE INTENTIONALLY LEFT BLANK

LIST OF ABBREVIATIONS, ACRONYMS, SYMBOLS

A_{MC}	Area of the Mini Cylinder Can
APC	American Piezo Ceramics
A_{PZT}	Area of the PZT stack
B&K	Brüel & Kjær
C_C	Coupling Capacitance
C_P	Preamp Capacitance
D	Electric displacement vector
$d\xi$	displacement of element *dx*
dx	infinitesimal element of PZT
e_n	Equivalent input noise of the preamp
e_s	Equivalent input noise of the source
FET	Field Effect Transistor
FFVS	Free Field Voltage Sensitivity
$\vec{\vec{g}}_{ij}$	Piezoelectric voltage coupling matrix (3x6)
JFET	Junction FET
k	Wavenumber
kT	Boltzmann thermal energy
ℓ	Length of the PZT bar
MCC	Mini CylinderCan
m_b	Mass of the PZT bar

m_L	Mass at free end of bar
OCV_{PZT}	Open Circuit Voltage intrinsic to the PZT material
$\vec{P}$	Polarization vector
PZT	Lead Zirconate Titanate
rtHz	Square root of bandwidth in Hz
R_d	Drain resistance
$\vec{s}_{ij}^{D}$	Elastic compliance matrix at constant displacement field vector
t	Thickness of the PZT
Y_{33}^{D}	Longitudinal Young's modulus under constant displacement field
USD	United States Dollars
ρ	Volume density
ρ_L	Linear density

ACKNOWLEDGMENTS

I would like to express my proud and excitement of completing this challenging and valuable part of my education here at the Naval Postgraduate School. I was really honored to be one of the students of this university and more particularly of the Physics department.

I would like to express my appreciation to my advisor Thomas J. Hofler from the Physics Department for the valuable knowledge he offered me with patience and detail. I would like to thank him for inspiring me in learning, trying harder and insisting on the well studied and carefully premeditated course towards the accomplishment of a goal. Thanks to George, Glenn and Sam for their technical support during this effort.

I would like to thank the persons who have embraced me and supported me all my life with love and understanding, my parents, for the difficult and responsible role of raising me with ideals and principles in a love-bonded family.

Finally I would like to thank my beloved wife Matina who followed me here, standing near me and encouraging me when I needed it most. I would like to thank her for proving me that love can be powerful and really inspirational!

THIS PAGE INTENTIONALLY LEFT BLANK

I. INTRODUCTION

A. BACKGROUND

During the last half century, the development of electroacoustic transducers in underwater acoustics, has been based on the well-known piezoelectric materials that converted the captured sound to electric energy, or reversely, the outgoing signal to acoustic energy. These elements are the most favorable and effective, and their crystallographic structure is related to their ability to transform energy. Their performance is also the result of their chemical composition. This results in three properties that are extremely useful in a transducer operation: linearity, passivity and reversibility. Among other ceramics, PZT or lead zirconate-lead titanate ceramics, exhibit exceptionally high electromechanical coupling coefficients, which represent the ratio of transduced to incoming energy. Of course, the former transduction properties result from a specific poling process, during which electrostrictive material properties are converted to piezoelectric properties under the stress of high electric fields and elevated temperatures. As little progress has been achieved in developing new polycrystalline ceramic compositions in recent years, great efforts have been expended in refining the production techniques and the design concepts for underwater projectors or hydrophones in a manner that could be used to improve the device's performance.[1]

Many underwater acoustic applications require the use of a device characterized by low noise as well as high sensitivity along with a broadband and flat response. In order to achieve such characteristics, the piezoelectric transducers usually have low impedance and high capacitance for reasons stated in Chapter II. Nevertheless, environment is an overriding factor, which influences the general concept of a hydrophone's design. Its effects appear in the form of noise, corrosion and disorders in the sound transmission.

It is well understood that noise is a limiting factor in the detection of signals. Therefore, hydrophones are frequently built to optimize the signal to noise ratio, or in other words, produce as low as possible self noise expressed as an equivalent noise sound

[1] O. B. Wilson, *Introduction to Theory and Design of Sonar Transducers*, Peninsula Publishing, Second Edition, 1988, pp. 2, 66, 73.

pressure. These devices not only achieve noise diminution at its transduction source, but they also work against subsequent effects, such as triboelectric and strumming noise. The triboelectric effects are usually found in the cable of the hydrophone, due to the motion of the cable and from the friction between the conductor and its shield when the cable is bent.[2] Strumming is a noise phenomenon related to the hydrophone's cable. Strumming noise is created by the vortices as the water flows past the cable causing it to vibrate, which in turn imparts acceleration to the sensing unit.

The use of a signal preamplifier is one of the common methods that can constrain the noise level and protect the detected sound signal quality as it is transmitted to some signal analyzers aboard a platform. Numerous modern designs include a preamplifier adjacent to the sensing material for a couple of reasons briefly mentioned later. Nevertheless, the classification of amplifiers should be mentioned depending on the manner in which the active device is operated.[3] Voltage preamplifiers are the sole concern of this thesis.

First, a satisfactory amplification stage ensures the existence of high input impedance. This is very accommodating, since it is important that the sensing element have a low impedance compared to the input impedance of the preamplifier. Secondly, the preamplifier should have the lowest possible output impedance compared to the impedance of the transmission cable including its distant termination.

The existence of a capacitance in parallel with a hydrophone causes a reduction in sensitivity. Consider a hydrophone having no preamplifier and the effect of its cable. If the hydrophone's sensing element capacitance falls to a value comparable to the cable, then the sensitivity decrease is quite significant.[4] Consequently, if a preamplifier is included in the hydrophone, the preamplifier's input capacitance should be made small compared to the capacitance of the PZT material.

---

[2] D. Stansfield, *Underwater Electroacoustic Transducers*, Bath University Press and Institute of Acoustics, 1990, p. 321.

[3] Neil Storey, *Electronics A Systems Approach*, Addison-Wesley, Second edition, 1998, p.323.

[4] D. Stansfield, *Underwater Electroacoustic Transducers*, Bath University Press and Institute of Acoustics, 1990, p. 294.

The preamplifier should have an output impedance that is low enough and an output current capacity that is high enough to drive the cable capacitance over the frequency range of interest. The total capacitance of the cable is related to its total length and the capacitance per unit length. Since the connection of the preamp with the cable is considered to be in parallel, the effect of the cable capacitance is to create a roll-off effect of the gain of the system, usually at a frequency above the bandwidth of interest. This high frequency cut-off can usually be one of the reasons for instability especially at the circuits with feedback arrangements.

Several construction methods, as well as various materials, have been used to ensure the proper insulation of hydrophones when submerged. The desired operational depth and the deployment time prospect are key points in the design. Characteristic examples are PZT ceramics embedded in fluid such as oil[5] or relatively massive metal housings used to satisfy, among other reasons, the necessity of keeping the ceramic away from water. Since water can be an aggressive solvent, especially with the passage of time, and can even migrate through plastics, materials such as polyurethane have been used to seal the entire piece of equipment. Polyurethane encapsulation is convenient and adequate for modest time periods of water exposure, though it is not suitable for long term exposure.

Furthermore, the shape of a transducer is an exact result of the expectations for a particular sound detection or projection capability. If the detected sound is very weak, the existence of the preamplifier is necessary, and therefore, a larger apparatus might be required. Another example is the famous Tonpilz projector. Tonpilz is German for "singing mushroom"[6] which was designed to deliver maximum output power. A large output power is associated with a greater volume velocity on the radiating face. Tonpilz's large radiating face increases the volume velocity for a given strain of the transduction material. By increasing the radiating surface, better impedance matching is also achieved between the water and the transducer. This is important for maximum output power.

---

[5] Certain types of oils like castor oil are acoustically similar to water but also are dielectrics.

[6] O. B. Wilson, *Introduction to Theory and Design of Sonar Transducers*, Peninsula Publishing, Second edition, 1988, p. 111.

The frequency bandwidth and the estimated quality of sound that the designer wishes to capture are also basic parameters to consider for a hydrophone. The balance between these two factors can drastically alter the construction. The performance of the previously studied hydrophone models which behaved very smoothly and with a very low noise level up to a frequency of 18-20 kHz led to the design studied in this thesis. The contribution of this study transferred the flat response up to 40 kHz with increased noise level, which will be discussed later.

Amid other issues, cost emerges, as always, as an important consideration when building a hydrophone. Commercial high quality hydrophones, such as those tabulated below, can cost over $500 with the majority valued at over $2,500.[7]

Hydrophone	***Receiving Sensitivity (db re 1V/ μ Pa)***	***Equivalent Noise Pressure Level (dB re 1 μ Pa/Hz$^{1/2}$)***	***Frequency Span***	***dB Variation***	***Dimensions***
Brüel & Kjær (B&K) 8103	-211.7	N/A	0.1Hz – 100 kHz	-1.5 +2.5	50mm x 9.5mm dia
Brüel & Kjær (B&K) 8106	-174	30	10 Hz – 40 kHz	+3 -1.5	182mm x 32mm dia
Reson TC4032	-170	29.5	5Hz- 85kHz	+1.5 -3	244.5mm x 38mm dia
Sensor Technology Ltd SQ-03	-162	N/A	1Hz – 65kHz	N/A	152.4mm x 25.4mm dia

Table 1. Competitive Commercial Hydrophones and Some Characteristics

[7] Bruel & Kjaer, Available [online] at [http://www.bk.dk], accessed March 4, 2004, Reson Inc., Available [online] at [http://www.reson.com], accessed March 5, 2004, and Sensortech, Available [on line] at [http://sensortech.ca], accessed March 5, 2004.

B. MOTIVATIONS

Every aspect of the design has been emphasized by Professor Thomas Hofler and various students of the Naval Postgraduate School (NPS) while designing and constructing previous hydrophones, called "MiniCans", in order to achieve most of the desirable characteristics. The MiniCan design was originally created with a nominal outer diameter of 1" and basically consisted of two rigid cylindrical parts made of aluminum 6061-T6 assembled one inside the other and separated by a small gap.[8] Inside the can, a pair of PZTs provided the sensitivity response and a flexible preamplifier was inserted in the available annular space inside the aluminum can. During this effort, six hydrophones were built and tested with improving performance resulting in MiniCan #6 which turned out to be outstanding. The achievement was a very low noise performance, exhibited by a small 0.90" maximum dimension device at very low cost. Its overall size has been reduced, since the nominal outer diameter of the aluminum can was just 0.66" (16.76mm). The achievement of a small hydrophone size can lead to omni-directionality and a high frequency response.

The total mass was decreased affecting the resonance frequency of the system which shifted to a higher region. The PZT used were changed from Navy type II to Navy type I, an essential alteration that ensured a lower noise performance. Furthermore, the developed flexible amplifier revealed an extremely good noise performance of $1.75 nV/Hz^{1/2}$ at 1 kHz, with a gain of approximately 18dB. The high resistance component ($100 M\Omega$), used as the input impedance of the preamplifier for the previous MiniCan models, has been replaced by an even larger ($1 G\Omega$), resistor. The Free Field Sensitivity of MiniCan #6 was measured to be -167.9 dB re $1 V/\mu Pa$ with a flat frequency response up to 20 kHz. In addition, the measured results for the sensitivity were very close to the theoretical values lagging only by a small difference of 1.4 dB. The agreement between theory and measurement was a consequence of a significant change in the design of the internal shape of the aluminum parts.[9]

---

[8] Miguel Alvarado, *Construction and Testing of Low Noise Hydrophones,* Master's Thesis, Naval Postgraduate School, 2003, p. 5.

[9] Ibid., p. 37.

However, it would be valuable to take advantage of the previous successes and focus on some of the problems that arose so as to fully understand the purpose of the present effort. Although the frequency response of the MiniCan is very good, the limitation of the upper frequency below 20 kHz cannot be ignored. In addition, the input capacitance value of the preamplifier was high, probably due to the Miller effect. Since the preamplifier is based on a JFET as its first amplification stage, the capacitances that exist in the JFET cannot be neglected.

Temperature was another factor that could have influenced the operational gain of the preamplifier. Ocean temperatures may vary by more than 20° C. A crude measurement with the simple non-feedback preamplifier used in the MiniCan indicates a gain variation in excess of 2 dB with respect to a temperature change of 20° C. For more critical applications where absolute signal strength measurement is required, this is probably unacceptable.

Finally, an additional drawback of the flexible preamplifier was the cost of its polyimide printed circuit board (PCB). (The "PCB" in this case is a thin flexible strip rather than a rigid "board" and is more expensive).

The major goals of this thesis follow.

- To construct and test two hydrophones, called the CylinderCan, based on a new model. The improvements include a flat response up to higher frequencies, a relatively low noise performance and better omnidirectionality.
- To improve and test a new rigid feedback preamplifier that would provide stable gain and less distortion.
- To keep the total cost as low as $50, similar to the cost of the models previously built.

However, are these improvements meant to be the only ones resulting from this preamplifier? Many more interesting facts will be revealed in subsequent chapters.

The author of this thesis was involved in the construction and analysis of the performance of these hydrophones. The concept, however, belongs to Professor Thomas Hofler of the Physics Department of the Naval Postgraduate School.

II. THEORY AND DESIGN

A. THEORY

The subminiature Mini CylinderCan hydrophones were designed and built for use as broadband frequency and low noise sensors. The performance of Mini CylinderCan units #1 and # 2, which hereafter are called MCC 2-1 and MCC 2-2, justify their extremely small dimensions. The shrinking of the sensor's size results in the extension of the upper frequency response limit and enables the representation of their behavior as acoustic lumped elements. Since the sound wavelength in the water is much greater than the MCC's dimensions (diameter of radiating face) for frequencies below 100 kHz, the characterization as lumped elements is sound and a simpler theoretical approach would be adequate to understand its performance. A basic consideration that stimulated the MCC design was that broadband hydrophones, such as those used in passive sonars, are preferred to avoid the marked variations of response that occur near the resonances. They are required to have uniform sensitivity over their bandwidth. The power they handle is small and, therefore, the electric-to-acoustic conversion efficiency is somewhat less important than in active sonar systems.[10] Had the dimensions been greater than the quarter of sound wavelength, diffraction effects might occur.

Hence, further study and testing was done by selecting a long cylindrical shaped hydrophone body, motivated by the desire to simplify the resonance frequency structure at 20 kHz and above. The original MiniCan's[11] design is a classic double piston configuration that is not quite symmetric about a plane through the mid-point. For this reason, in addition to possible diffraction effects, the response of the MiniCan can be erratic for frequencies above 10 kHz. On the contrary, MCC uses a single piston, since the backside of the sensing material is fixed. Then there is no longer any acoustic

[10] In contrast, projectors need much more power, thus they have to operate near their resonance. D. Stansfield, Underwater Electroacoustic Transducers, Bath University Press and Institute of Acoustics, 1990, pp. 2 and 279.

[11] S. Polydorou, A Compact and Inexpensive Hydrophone Having Ultra Low Self-Noise, Master's Thesis, Naval Postgraduate School, Monterey, California, 2002, p. 3.

cancellation, as in the case of two sensing pistons. The longer hydrophone body was also necessitated by a new preamplifier design that is currently being fabricated on a rigid PCB (as opposed to a flexible PCB) for reasons of cost.

A beneficial result emerges from designing a small hydrophone. It is known that the performance of a hydrophone is usually expressed by the free field sensitivity or the pressure sensitivity.[12] In the case of device dimensions that are small compared to a wavelength, the two measures of sensitivity are almost equal.

A primary resonance frequency can be determined by expressing a simple theory that simulates the MCC operation. The entire system can be represented as a system of a mass loaded bar having one fixed end. If the mass of the cylindrical body is assumed much larger compared to the mass of the PZT stack and to the mass of the lid, then the PZT stack and lid model can be assembled on a rigid wall without any loss of generality. The mass of the stack m_b contributes to the total vibrating mass since it is comparable to the mass of the lid m_L. Moreover, the PZT stack can be represented by a rod that vibrates longitudinally as force acts on the attached mass. This applied force represents the sound pressure being sensed by the hydrophone. The following figure describes the system.

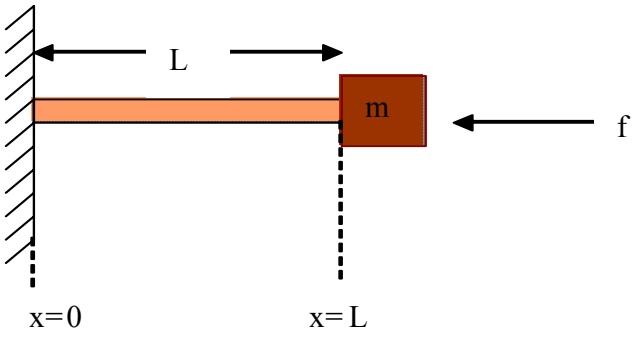

Figure 1. Mini CylinderCan Design Acting as a Mass-Loaded Fixed Bar

[12] Free field sensitivity is the ratio of output voltage to the applied sound pressure when the output is open circuited; the output voltage is referred to acoustic pressure that would exist in the place of the hydrophone when the hydrophone is absent from the field. Pressure sensitivity relates the output voltage to the actual acoustic pressure at the face of the sensor.

The PZT bar is modeled as an elastic element having a mass per unit length given by ρ_L. The primary frequency of the system can be defined by using the theory of vibrations of bars for a fixed – mass loaded bar[13]. In the case of no internal losses in the bar, the wave equation is

$$\frac{\partial^2 \xi}{\partial x^2} = \frac{1}{c^2}\frac{\partial^2 \xi}{\partial t^2} \tag{2.1}$$

for the mass *dm* of the segment *dx*. The complex harmonic solution of the displacement will be $\xi(x,t) = \mathbf{A}e^{j(\omega t - kx)} + \mathbf{B}e^{j(\omega t + kx)}$, where **A**, **B** are complex amplitude constants and *k* the wave number. Since the force at the right end is compressive,

$$\mathrm{f}_L = -S \cdot Y_{33}^D \cdot \left(\frac{\partial \xi}{\partial x}\right)_{x=L} \tag{2.2}$$

where S is the cross sectional area of the bar and Y_{33}^D the longitudinal Young's modulus under constant displacement field and $\left(\frac{\partial \xi}{\partial x}\right)_{x=L}$ is the strain of a segment of the bar (differential change in length over its original length *dx*) at the end of it. Then the boundary conditions at x=0 is that the displacement should be zero $\xi(0,t) = 0$. This yields

$$\xi(x,t) = -2jA\sin(kx)e^{j\omega t} \tag{2.3}.$$

At x=L, the applied force leads to an acceleration of the right end

$$\mathrm{f}_L = m_L\left(\frac{\partial^2 \xi}{\partial t^2}\right)_{x=L} \tag{2.4}.$$

Since $\left(\frac{\partial^2 \xi}{\partial t^2}\right)_{x=L} = 2j\omega^2 A\sin(kx)e^{j\omega t}$ and $\left(\frac{\partial \xi}{\partial x}\right)_{x=L} = -2jkA\cos(kx)e^{j\omega t}$, the result of the second equation will be $2m_L j\omega^2 A\sin(kx)e^{j\omega t} = 2jk\cos(kx)e^{j\omega t} S \cdot Y_{33}^D \Rightarrow$ $m_L\omega^2\sin(kL) = S \cdot Y_{33}^D \cdot k \cdot \cos(kL) = S \cdot c^2 \cdot \rho \cdot k \cdot \cos(kL)$. If the total mass of the bar is

[13] L. Kinsler, A. Frey, A. Coppens, J. Sanders, Fundamentals of Acoustics, J. Wiley & Sons, Fourth edition, 2000, p. 75.

$m_b = \rho_L \cdot L$, where the density per unit length is $\rho_L = S \cdot \rho$ and $\omega = c \cdot k$, the relation becomes $\cot(kL) = \frac{m_L \omega^2}{S\rho c^2 k} = \frac{m_L c^2 k^2}{\rho_L c^2 k} = \frac{m_L}{\rho_L} k = \frac{m_L}{\rho_L L} kL$. The final equation is

$$\cot(kL) = \frac{m_L}{m_b} kL \tag{2.5}$$

This equation is transcendental and the solutions are computed using Excel assuming that the first solution is found in the region $0 < kL < \pi$. Since $k = \frac{\omega}{c} = \frac{\omega}{\sqrt{\frac{Y_{33}^D}{\rho}}} = \frac{2\pi f}{\sqrt{\frac{Y_{33}^D}{\rho}}}$, the resulting resonance frequencies are

$$f = \frac{\sqrt{\frac{Y_{33}^D}{\rho}}}{2\pi} k \tag{2.6}$$

The presence of the urethane on the lid has to be calculated as an additional mass on the mass of the lid. Furthermore the water radiation mass should be included in the vibrating mass.

While treating MCC as a tube with a piston at its end, the radiation impedance of water must be considered. More specifically, the radiated energy can be split in two quantities: the energy radiated in water or water resistance and the energy stored (reactive) and returned back to the system. Thus, the water impedance can be represented by a resistive and a reactive component as $Z_r = R_r + jX_r$. These variables can be studied by equivalent mechanical circuits (R_M and X_M) which contribute to the mathematical solution of the radiation impedance. As demonstrated in Figure 2 there is a change of the reactive and resistive part as the quantity *ka* changes. The quantity *ka* represents the relation between the piston diameter and the wavelength. When *ka* is smaller than about 1.6 the reactance X_M dominates over the resistance and changes by the first power of frequency while R_M changes by the second power of frequency. In this case the fluid acts

like additional mass, called radiation mass. The size of this mass can be estimated by a cylinder of water of area $\pi\alpha^2$ and length 0.85a, in the case that the piston is considered an unbaffled piston.

$$M_{rad.water} = (0.85 \cdot \alpha) \cdot \pi \cdot \alpha^2 \cdot \rho_{water} \tag{2.7}$$

The following figure[14] illustrates the aforementioned observations:

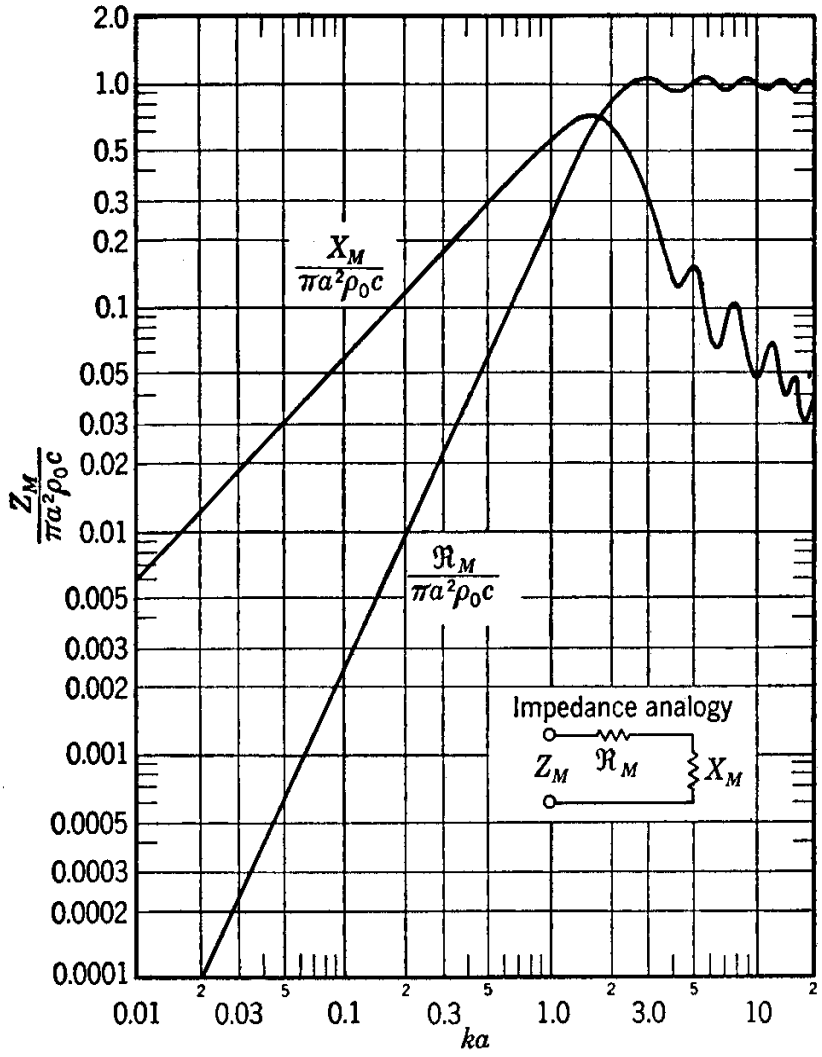

Figure 2. Real and Imaginary Parts of the Normalized Mechanical Impedance of the Fluid Load Upon a Piston of Radius *a* Mounted in the End of a Long Tube

[14] Ibid., p.122.

The data used for the theoretical calculations can be found in the following table:

Used variables	*MCC 2-1*	*MCC 2-2*
Longitudinal Young's modulus	$1.09 \cdot 10^{11}$ N·m^2	$1.08 \cdot 10^{11}$ N·m^2
PZT Density	7600 kg/m^3	
Thickness of PZT stack	4.064 mm	4.128 mm
Mass of lid	0.1247 g	0.17 g
Average diameter of radiating surface	6.985 mm	6.9406 mm
Average height of urethane on lid	0.762 mm	0.635 mm
Density of urethane	1.08 g/cm^3	
Mass of urethane on lid	0.0325 g	0.02576 g
Water Radiation mass	0.114 g	0.1116 g
Total vibrating mass	0.27 g	0.3075 g

Table 2. Data Used in Resonance Frequencies Calculation

The longitudinal Young's modulus under constant dynamic component of electric field *E*, Y_{33}^E, usually can be found in the specifications sheet provided by each manufacturer. However the Young's modulus under constant displacement field *D*, Y_{33}^D, is not provided. A nice way to calculate this quantity is based on some of other known properties of the ceramic such as the free dielectric constant K_3^T, the dielectric permittivity of vacuum ε_o ($8.85 \cdot 10^{-12}$ F/m) and the piezoelectric strain constant d_{33}. For these calculations the measured d_{33} for each PZT was used to improve the accuracy. Thus the Young's modulus under constant displacement field *D* is given by

$$\frac{1}{Y_{33}^D} = \frac{d_{33}^2}{\varepsilon_3^T} - \frac{1}{Y_{33}^E} \tag{2.8}$$

where ε_3^T is the dielectric permittivity under constant stress given by $\varepsilon_3^T = K_3^T \cdot \varepsilon_o$. The calculated Y_{33}^D for each stack is listed in Table 1. The measured d_{33} for each stack is provided below

PZT	d_{33} *(pC/N)*	*Remarks*
#1 and #3	325	Used in MCC 2-1
#2 and #5	327	Used in MCC 2-2

Table 3. Measured d_{33} for the Ceramics Used in MCC

The above theory predictions for the MCC 2-1 and MCC 2-2 are tabled below:

	MCC 2-1	*MCC 2-2*
kL for first resonance	1.01	0.975
First Resonance frequency	149.8 kHz	141.7 kHz

Table 4. Resonances Frequencies for MCC 2-1 and 2-2

It is evident that the resonant frequencies from the longitudinal vibration of the sensing element are far above the upper limit of the operational bandwidth of hydrophones.

The aluminum lid was purposely designed to be light and have small mass inertia, and thus accurately "transmit" the variations of the incident pressure waves. If more mass is added to the lid, the hydrophone becomes more acceleration sensitive. Another reason for considering the thickness of the lid is its flexural resonance. For qualitative purposes, the lid can be represented with a thin square vibrating plate of side *a* and thickness *t*.

The theoretical flexural resonance frequency of this plate is given by[15]

[15] O. B. Wilson, Introduction to Theory and Design of Sonar Transducers, Peninsula Publishing, Second edition, 1988, p. 114.

$$f_r = \frac{14.1}{2\pi \cdot a^2}\sqrt{\frac{Y \cdot A \cdot t^3}{12m(1-\nu^2)}} = \frac{14.1}{2\pi \cdot a^2}\sqrt{\frac{Y \cdot t^2}{12\rho(1-\nu^2)}} \tag{2.9}$$

where Y is the Young's modulus, ρ the mass density, A the vibrating surface and v the Poisson's ratio. The edges of the plate are assumed to be free and the center of the plate is assumed to be a node of the vibration. It should be mentioned that the relationship between frequency and thickness is linear, and so if the thickness is doubled, the frequency will double. This result might be considered because the flexural stiffness should increase as the cube of the thickness and the frequency increases with the square root of the stiffness. However, the increase of the mass of the lid is proportional to the thickness. Obviously, it would be more convenient if the resonances increase faster than a linear relation to thickness, but they do not. Therefore, MCC 2-2 was designed with a more massive lid in order to increase its flexural frequency.

The open circuit sensitivity is one of the fundamental acoustic quantities for which the theoretical calculation based on the piezoelectric transduction equations yields a prediction.[16] There are certain stimuli and response variables involved and some must be chosen as independent. Depending on the assumed electrical load, the analysis is different for an infinite input electrical impedance which represents a voltage amplifier and the zero input impedance corresponding to a charge amplifier. In the case of MMC, which uses a voltage amplifier, the dynamic component of the variables Q (charge) and D (electric field displacement) are considered zero.

The expected stress tensor is $T = \begin{pmatrix} 0 \\ 0 \\ -T_3 \\ 0 \\ 0 \\ 0 \end{pmatrix}$. Thus, the piezoelectric relations that may be useful are $\begin{Bmatrix} \vec{S} = \overleftrightarrow{s}^D \vec{T} + \overleftrightarrow{g}_t \vec{D} \\ \vec{E} = -\overleftrightarrow{g}\vec{T} + \overleftrightarrow{\beta}^T \vec{D} \end{Bmatrix}$ Then, in accordance with the above assumptions:

[16] Ibid., p. 57.

$$\vec{E} = -\overleftrightarrow{g}\ \vec{T} = -\begin{pmatrix} 0 & 0 & 0 & 0 & g_{15} & 0 \\ 0 & 0 & 0 & g_{15} & 0 & 0 \\ g_{31} & g_{31} & g_{33} & 0 & 0 & 0 \end{pmatrix} \begin{pmatrix} 0 \\ 0 \\ -T_3 \\ 0 \\ 0 \\ 0 \end{pmatrix} = -\begin{pmatrix} 0 \\ 0 \\ -g_{33}T_3 \end{pmatrix} \Rightarrow E_3 = g_{33}T_3 .$$

It is known that for the generated electric field E_3, the sensing voltage will be $V = E_3 \cdot t = g_{33}T_3 \cdot t$, where t is the PZT thickness between electrodes, and the voltage sensitivity to the stress T_3 is

$$OCV = M_V = \frac{V_{out}}{T} = g_{33} \cdot t \tag{2.10}$$

The open circuit sensitivity (OCV) is used to express the intrinsic capability of the sensor to produce a certain amount of voltage under a certain applied stress and also is used as an important measure of the merits of a design.

The Mini CylinderCan design takes advantage of the relatively high sensitivity derived in (2.13) and improves its performance further by using two PZT parts. Due to the parallel electrical connection of the ceramics, the voltage sensitivity remains unchanged while the stack capacitance is doubled. In this way the achieved sensitivity is retained and at the same time the noise performance is improved by the higher capacitance.

According to the theoretical formula, the free capacitance for the cylindrical PZT is $C_f = \varepsilon_{33}^T \cdot \frac{\pi \cdot a^2}{t}$, where α is the radius of its base and t its thickness. The theoretical prediction for the free capacitance of each PZT is 71.6 pF taking in account the PZT diameter 2α=4.064 mm and thickness t=2.045 mm. The total free capacitance of the stack is predicted to be 145.9 pF.

B. BASIC MINI CYLINDERCAN DESIGN

The electro-acoustic sensor consists of two ceramics forming a stack, fitted in a cylindrical body and covered by an aluminum lid. The entire structure was made waterproof with the help of polyurethane, a flexible material suitable for transmitting the

stresses of underwater dynamic pressure to the aluminum lid. MCC 2-1 has a preamplifier tube of uniform thickness, while MCC 2-2 has a thinner wall at the bottom part, in an effort to increase the fundamental resonant frequency of the tube. As mentioned previously, by increasing the mass at the end of the tube, the approximation of the rigid wall can be valid. The thinner lower part ensures that the mass of the tube there is not so large, and the aluminum fitting mass is low, keeping the resonance of the tube high. The cable, the preamplifier, the metal mounting parts and two electrodes of the PZTs all form a common electrical ground. An electrode was placed between the two PZTs sensing the EMF's generated there and conveying them to the preamplifier input.

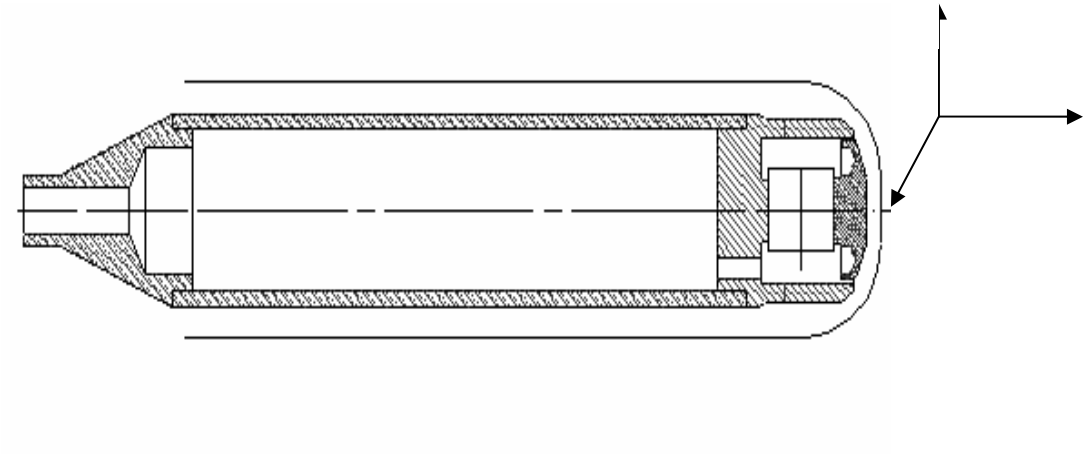

Figure 3. Mini CylinderCan Design

The cylindrical shape of the body accommodates the intention to achieve a very good omnidirectional response in the horizontal plane (1 and 2 directions in Fig. 3), a reasonably omnidirectional response in the vertical plane. Whenever a change in pressure occurs, the water volume deformation induces a certain alternating pressure on the aluminum cap. Thereafter, this excitation travels to the adjacent PZT surface. In this way, only the longitudinal polarization is activated and the PZT senses the pressure only along the *z* or *3* direction.

It is possible to reduce the ceramics' radial constraints by machining the inner part of the main body with a circular step rising at the lower part of the main body and on the aluminum lid. A failure to minimize radial constraint of the ceramic will result in a sensitivity that a considerably less than that derived in Eq. (2.13). The building material

for the main body was stainless steel because the high modulus should make it rigid relative to the acoustic impedance of water and the higher density should help keep the body stationary.

The ceramics that receive incident pressure in just one lateral surface may give insufficient sensitivity. Thus, there can be an amplification of the voltage signal by a mechanical transformation. Specifically, a mechanical leverage or stress amplification can be employed, whereby the stress in the ceramic is much higher than the acoustic pressure in the water. Quantitatively, the stress amplification is given by the ratio of $\frac{A_{lid}}{A_{ceramic}}$, and the more open circuit sensitivity is increased by this factor. A_{lid} stands for the cap's area and $A_{ceramic}$ for the PZT electrode surface area. The Mini CylinderCan's lid diameter is about 65% bigger than the PZT diameter. Therefore, it is possible to predict increased sensitivity by a factor of 2.96 for MCC 2-1 and 2.83 for MCC 2-2.

C. MINI CYLINDERCAN 2-1

This unit was the first one constructed and consists of the following parts:

- Lid constructed of Aluminum 6061-T6
- Main body made of stainless steel
- Tube made of stainless steel
- Cable fitting made of stainless steel
- Twin-lead cable consisting of two wires and a braided shield (input, output, ground)

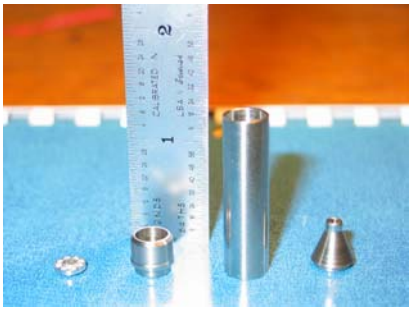

Figure 4. Mini CylinderCan Design Parts (left to right: lid, main body, tube, cable fitting)

The majority of these parts had been machined of stainless steel in order to take advantage of properties such as the steel's density, modulus, and sound speed which are relatively large and ensure high resonance frequency. The above combination satisfies the design's concern for a protective enclosure, not easily affected by the environmental vibrations and the hydrostatic pressure, and is also highly corrosion resistive. The lid was constructed of aluminum since it is lightweight and great efficiency was desired, especially for this part of the hydrophone that transfers the pressure's alterations to the PZT.

The following table describes the physical characteristics of each part.

Outer diameter of the lid	6.858	mm
Interior diameter of the main body	7.112	mm
Gap between main body rim & lid	0.125	mm
Outer diameter of the PZT	4.064	mm
Average diameter of lid	6.985	mm
Thickness of one PZT part	2.045	mm
Area ratio between diameter lid & PZT	2.96	---
Mass of the lid	0.1247	g
Mass of the main body , 2 PZT stack	2.85	g
Mass of the finished assembly	15.95	g
Measured capacitance of the PZT stack	157.8	pF
Capacitance of the rigid feedback preamp	9.3	pF
Gain of preamp	19.51	dB
Theoretical sensitivity w/ preamp gain	-177.86	dB re 1 V/μPa
Measured Underwater Pressure Sensitivity	-177.4	dB re 1 V/ μPa

Table 5. Main Characteristics of MCC 2-1

The formula mentioned in theory calculates the theoretical sensitivity $OCV = M_V = \frac{A_{lid}}{A_{ceramic}} \cdot g_{33} \cdot t$. It is essential also to take under consideration the signal attenuation due to the parallel capacitances of the ceramic and the preamplifier.

When calculating the total preamp capacitance, the capacitance of the protective diodes and the JFET effective capacitance are considered to be 4 pF and 3pF respectively. The stray capacitance that may exist in the preamplifier is also included and estimated to be about 7pF. The total stray plus preamp capacitance of 14.3 pF along with the ceramic capacitance 143.2 pF creates a 0.81 dB signal attenuation.

According to the PZT's the specifications sheet [17] $g_{33}=24.6\cdot10^{-3}[V\cdot m/N]$

$$OCV=\frac{A_{lid}}{A_{ceramic}}\cdot g_{33}\cdot t=\frac{r_{lid}^2}{r_{ceramic}^2}\cdot g_{33}\cdot t\Rightarrow$$

$$=\frac{d_{lid,average}^2}{d_{ceramic}^2}24.6\cdot10^{-3}[V\cdot m/N]\cdot2.045\cdot10^{-3}m=0.0537[V\cdot m^2/N]\left(\frac{6.985\cdot10^{-3}}{4.064\cdot10^{-3}}\right)^2=1.49\cdot10^{-4}[V/Pa]$$

Therefore, *OCV*= -196.56 dB re 1V/μPa and the net sensitivity is –196.56 dB + 19.51 dB – 0.81 dB = -177.86 dB re 1V/μPa.

Material preparation was necessary to ensure that the upcoming bonding procedure would be correct. Thus, every PZT was very gently sanded with sandpaper of silicon carbide (600 grit) at both the upper and lower base, providing a clean surface, purified of any oxide on the surface and ready for the epoxy (Emerson & Cumming Stycast 1266) to be applied. Also, the d_{33} constant was measured and the PZT's polarity was marked. Their measured capacitances were 80.2pF and 77.6 pF with the B&K Precision Universal LCR meter. Subsequently, copper foil was cut in the exact circular shape of the PZT with an extra tiny tab, so that the input wire of the preamp could be soldered to it.

All the parts were cleaned in order to provide for good epoxy bonding and electrical contact with an alcohol-based electronics solvent. The epoxy was prepared in the appropriate amount in order to use it for joining the two PZTs. Before joining the three parts (2 PZTs and the copper foil in between), two PZTs were selected that had the same charge constant $d_{33}=325\frac{pC}{N}$. This was convenient, since with the same charge constant and under the same amount of force, the PZTs would produce the same amount

[17] Morgan ElectroCeramics, Available online at http://www.morganelectroceramics.com/pzmat11.html accessed 01 June 2004.

of charge. The two ceramics were glued together with the polarizations oriented anti-parallel. Only a tiny drop of epoxy was used creating an extremely thin layer, which did not prevent the necessary electrical contact between the two sensing materials. The cure of the epoxy took place on a hot plate of 48°C, a temperature that does not cause depolarization ($T_{depolarization} \geq 100^{o} C$), but accelerates the process. The lower and upper part of the stack were protected by pieces of Teflon material, preventing the surfaces of the PZT' s from coming in touch with either the hot-plate or the pressing tool. The soft Teflon prevents brittle fracture of the PZT.

Figure 5. Stack of PZT Navy Type-I

The next step was to put the ceramic stack into the main body. The alignment tool was especially designed for this step and it helped to keep the stack in the middle of the main body. The clamping tool presses the PZT stack into the stainless steel body until the epoxy was cured.

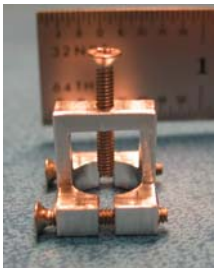

Figure 6. Clamping Tool

The wire that provides the lid's grounding had to be soldered at the inner part of the main body. Acid flux was selected for soldering to the stainless steel. The grounding wire was given a curvy shape to avoid contact with the preamp's input wire. The soldering iron temperature was approximately 540-560°F, and the soldering was performed on a hot plate (Thermolyn Cimarec 1) warmed to 136°C.

At this point, the preparation of the coaxial cable had to be completed. The cable used is a shielded twin-lead cable with two twisted wires (input/ output) and an outer braided ground wire, protected by a thick plastic jacket. Modern hydrophones usually have cables with insulation made of neoprene or polyethylene, but it was not possible to find such a cable with the desired diameter on the open market. The wires were cut at the exact length in order to be soldered without any bending or stretching. The tips of the wires were sanded and given a flat shape to make the soldering area larger. Thus, the solder bonding with the preamplifier became stronger. A minute amount of the KESTER SP-30 helped in soldering the wires on the preamplifier's board. Five-minute epoxy covered the joints to further increase their strength.

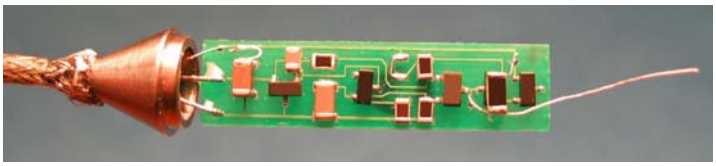

Figure 7. Cable Fitting and Wires Soldered to the Preamplifier

Thereafter, five-minute epoxy was applied to the cable fitting, the tube, and the body and a pressing tool was used to force all three pieces together. The procedure was executed in one step and an appropriate aluminum tool provided the suitable base for the entire assembly. Further care was taken while sliding the preamp's input wire through the insulated hole of the main body. The connected parts were cured on a hot plate (55-60^{o}C) for a day.

The grounding wire was inserted in one of the small dimples of the lid, half filled with an amount of silver epoxy, FS-339. Since silver epoxy is a bonding material that needs time to harden, a couple of curing days were essential. Further, the lid was adjusted on the body and with the support of four clear Mylar patches with a thickness of 5/1000", an equidistance was kept between the lid's edge and the body's periphery. Then GE Silicone RTV 615A was applied amid the aforementioned space. The RTV has a very soft hardness. The goal was the water isolation of the PZTs, and the cap's freedom of motion for pressure sensing.

The last series of construction steps dealt with the hydrophone's coating with polyurethane Devcon Flexane 80. A spinning lathe was used to pot the hydrophone with urethane. A heating source was placed close to the hydrophone until the urethane became hard enough to cure without sagging.

Figure 8. Hydrophone Spinning in the Lathe

The same material covered the rest of the body and efforts made to avoid trapping air bubbles, because of their potential to effect on the sensor's response. The weight of the final device was measured at 15.95 g.

Figure 9. Hydrophone Partially Covered with Polyurethane

Figure 10. Hydrophone Totally Covered with Polyurethane

D. MINI CYLINDERCAN 2-2

The second hydrophone built was designed with significant differences from MCC 2-1, some of which were already stated. As mentioned previously, the lid was

arranged to be thicker and more massive. The cable fitting was constructed of aluminum instead of stainless steel in order to reduce the total weight of the device. Its walls are thinner and the outer diameter is smaller than MCC 2-1. The tube is not uniformly thick, and exhibits the rigid end characteristic on one end (near the main body) and is mass loaded by the cable fitting. Both PZT parts used have measured capacitances of 78.7 pF each.

The following table describes the physical characteristics of each part:

Outer diameter of the lid	6.8072	mm
Interior diameter of the main body	7.074	mm
Gap between main body's rim & lid	0.1335	mm
Outer diameter of the PZT	4.128	mm
Average diameter of lid	6.9406	mm
Area ratio between diameter lid & PZT	2.83	---
Thickness of PZT	2.045	mm
Mass of the lid	0.17	g
Mass of the main body , 2 PZT stack	2.85	g
Mass of the finished assembly	12.04	g
Measured capacitance of the PZT stack	157.4	pF
Capacitance of the rigid feedback preamp	6.4	pF
Gain of the rigid feedback preamp	19.01	dB
Theoretical sensitivity	-178.7	dB re 1 V/μPa
Underwater Measured Pressure Sensitivity	-178.02	dB re 1 V/μPa

Table 6. Main Characteristics of MCC 2-2

Similarly, with MCC 2-1, the open circuit sensitivity is:

$$OCV = \frac{d_{lid,average}^2}{d_{ceramic}^2} \cdot g_{33} \cdot t = \left(\frac{6.9406 \cdot 10^{-3}}{4.128 \cdot 10^{-3}} \right)^2 \cdot 24. \cdot 10^{-3} [V \cdot m/N] \cdot 2.054 \cdot 10^{-3} m = 1.43 \cdot 10^{-4} [V/Pa]$$

Therefore, *OCV*= -196.9dB re 1V/μPa and the net sensitivity is –196.9 dB + 19.01 dB – 0.81 dB = -178.7 dB re 1V/μPa.

Another important factor taken into consideration was the acoustic effect of the hydrophone cable on the hydrophone's sensitivity. The existence of air bubbles between the various layers of insulation can alter the acoustic pressure field. A technique of impregnating rubber into the braid and in between the inner insulation of the central wires was used in order to eliminate the possibility of cable effects.

While building MCC 2-2, General Electric silicon rubber RTV 615 was forced into the cable for a length of about 1 m, thus the trapped air near the hydrophone and retaining the flexibility and softness of the cable. The effect of air bubbles can be very significant and have nonlinear effects on the acoustic field. The density and compressibility of a medium is altered and resonances can emerge when bubbles exist. Therefore, the entire construction process was afforded special consideration to avoid creating bubbles in any part of the device.[18] The interested reader can read more about the research on cables in a thesis written at the same time with the present one, that contributed to the analysis of such fields.[19]

The procedure in the construction of MCC 2-2 was the same as MCC2-1 but with the following modifications:

- Polyurethane partially covered the hydrophone in order to make it watertight. On the other hand only certain parts were covered in order to constrain any negative features, such as the introduction of bubbles around the hydrophone. In this way we decreased the chances of changing the acoustic field, and therefore, hydrophone's performance

[18] L. Kinsler, A. Frey, A. Coppens, J. Sanders, Fundamentals of Acoustics, J. Wiley & Sons, Fourth edition, 2000, p. 238.

[19] Mario Maggliocetti, Construction of Low Noise Hydrophones, Master's Thesis, Naval Postgraduate School, Monterey, California, 2004.

- The grounding braid of the transmission cable was stabilized on the inner walls of the fitting using silver epoxy, since the fitting is now aluminum and will not accept conventional solder.

Figure 11. Cable Fitting with Silver Epoxied Braid on its Inner Walls

Figure 12. Mini CylinderCan 2-2

THIS PAGE INTENTIONALLY LEFT BLANK

III. IMPROVED FEEDBACK PREAMP AND MEASUREMENTS

A. IMPROVED FEEDBACK PREAMPLIFIER DESIGN

1. Introduction

Several aspects must be scrutinized concerning the preamplifier's design. Gain, bandwidth, impedance levels, feedback and stability are some complementary factors to the noise performance under the scope of a low noise design. Motchenbacher and Fichen provide a further analysis of the low noise concept.[20] The featured preamplifier of this thesis is single ended with three stages of signal amplification. The first stage is a JFET, the second a common emitter and the third stage is an emitter follower with overall feedback incorporated across all three stages.

The previous approaches to this field started initially with a simple two stage single ended JFET circuit, used in the first MiniCan hydrophones, which developed into a three stage feedback arrangement for the MiniCan and Mini CylinderCan hydrophones.[21] The results were exceptionally good since the low noise level of 1.75 $nV/Hz^{1/2}$ was accomplished and the self noise pressure level was found to be less than or equal to the Wenz's minimum noise over most of the hydrophone's frequency span. Despite this outstanding behavior, some limitations emerged, such as a very limited input voltage range and output current above 5 kHz.

Due to the performance problems mentioned above were obvious, and because their cause was not understood at the time, only the general feedback preamp schematic and benefits were included in the Alvarado thesis. Once the performance problems were understood, a few small modifications were made to the design and tests were made. These changes and results are summarized below.

The new schematic of the improved preamplifier, shown in following figure, manages to overcome these obstacles and achieve a low noise level. However, the noise performance is a small amount higher than the previous design.

---

[20] C. D. Motchenbacher and F. C. Fitchen, Low Noise Electronic Design, J. Wiley –Interscience Publication, 1973.

[21] Miguel Alvarado, *Construction and Testing of Low Noise Hydrophones,* Naval Postgraduate School, Master's Thesis, 2003, p. 8.

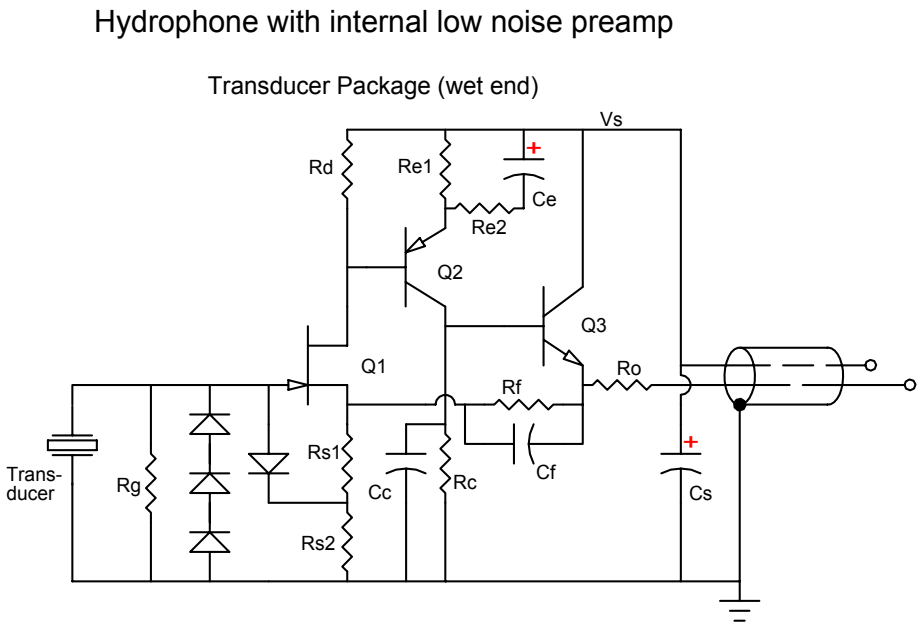

Figure 13. Feedback Preamplifier

A rigid printed circuit board (PCB) was used in an effort to reduce the production cost of the unit, at least at this developmental stage, and at the same time making this part more enduring and suitable for the cylindrical tube of the Mini CylinderCan hydrophone. Today's cost of a flexible PCB on the market is estimated around $6.50 and that of the rigid at only $1.60.

2. Low Noise Design

The selection of single-ended input and output preamplifier was preferred because it is simpler and inherently lower in noise than a differential input preamplifier. The alternative solution is the utilization of differential amplifiers that frequently form the foundations of modern opamp circuits. In the latter schemes, it is desirable to reject common mode input signals and respond only to the differential mode signals, as in the case of long input cables connecting a sensor with an amplifier.[22] In this project however, the employment of a differential amplifier could generate extra noise since the preamp can contribute an equal amount of noise in each of the two inputs, which of course, is added and results in a 3 dB increment of output noise (doubling of noise power). Furthermore, the construction a discrete component amplifier facilitates the transistors'

[22] Neil Storey, *Electronics A Systems Approach*, Addison-Wesley, Second Edition, 1998, p. 89.

selection for each stage, according to their particular noise performance. Thus, the preamp corresponds to a better noise level of roughly 8 to 15 dB than modern low noise opamps. However, in spite of the significant differences, the preamplifier of Fig.13 does resemble an opamp with a negative feedback and with its input terminal behaving as the non-inverting input of an opamp.

The feedback feature was very valuable in various performance details related to gain, input voltage, output current, distortion effects, and input impedance. An ideal voltage preamplifier would draw no current from the source and would give an output independent of the load. Hence, the ideal situation is approximated only if the input resistance of the preamplifier is extremely large, its input capacitance is very low and the output resistance tends to be zero. If the effects of these impedances can then be considered negligible, a maximum gain would be obtained.

A good starting point for such a preamp is to select a JFET instead of a BJT as a first stage transistor since it has an extremely large input impedance (~10^{12} Ohms) and low input current. This is particularly important for small broadband piezoceramic sensors, where the low frequency signal source impedance may be in excess of 10 MΩ. Using a BJT for the first stage would create a large input bias current and a correspondingly large input noise current. The combination of the high source impedance and large input noise current would result in very poor noise performance.

3. Stabilizing the Gain with Respect to Temperature Variations

In addition, the role of the feedback for a voltage amplifier is advantageous, since it stabilizes the voltage gain. This was the original motivation for the feedback design. A change in temperature influences the transconductance of the JFET, g_m, and this in turn influences the first stage gain

$$A = \left(\frac{1}{1 + \frac{1}{g_m R_s}} \right) \frac{R_d}{R_s} \tag{3.1}$$

where R_d is the drain resistor and R_s is the JFET source resistance. Thus the change of temperature used to affect the preamplifier gain by altering the first stage gain. With the new more sophisticated design, changes in temperature do not affect the gain of the preamp since now the gain is given by the formula

$$A = 1 + \frac{R_f}{R_s} \tag{3.2}$$

where R_f the feedback resistor. In this way the gain become independent of the transconductance of the JFET and thus is stable. This general gain stability problem is perhaps more important than it seems since variations in ocean temperature can be large.

4. Increasing Large Signal Clipping Limits

The achieved output current of earlier work[23] was of the order of 0.4 mA while the maximum output current for this feedback amplifier is higher by a factor of 8, reaching up to 3 to 4 mA. Most of the large third stage current flows through the feedback resistor R_f and the source resistor R_{s1} and R_{s2}, which lifts the DC voltage of the JFET source significantly higher, but not so high that it would force the JFET to stop functioning. The higher source voltage leads to the capability of receiving larger input signal voltages. In this way, both larger input voltage amplitudes and larger output current amplitudes are achieved.

5. Reducing the Miller Effect and Input Capacitance

The expected advantages of using the feedback feature were the stability of gain and the lower distortion of the preamplifier. However some interesting and very valuable improvements in preamp performance were found to be associated with the feedback design.

Another significant benefit of the use of feedback is the lowering of the input capacitance of the preamplifier. As an example of a typical Miller effect, consider the simple JFET preamp used in the MiniCan hydrophone, and shown below in Fig. 14. The first stage is a common source JFET amplifier stage.

[23] Miguel Alvarado, *Construction and Testing of Low Noise Hydrophones,* Naval Postgraduate School, Master's Thesis, 2003

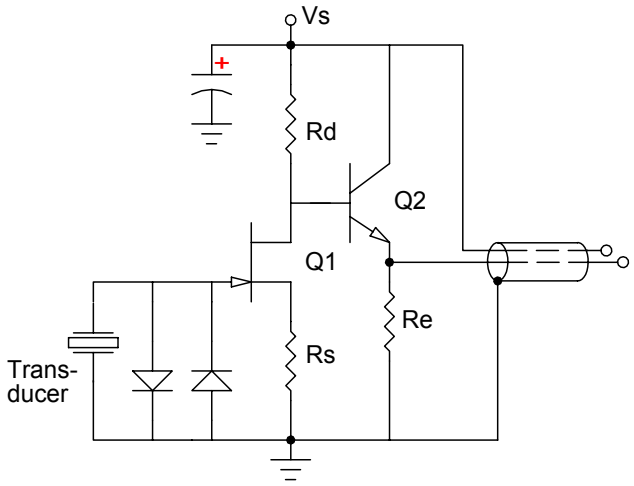

Figure 14. Simple 2 Stage Preamp without Overall Feedback. $R_d >> R_s$

The preamp input capacitance is generated by the gate to source capacitance C_{gs}, the gate to drain gain $A_{V,gd}$, and the gate to drain capacitance $C_{gd,}$ as shown:

$$C_{input} = C_{gs} + A_{V,gd} \cdot C_{gd} \tag{3.3}$$

The 2nd term in Eq. (3.4) is called the Miller effect. The gain $A_{V,gd}$ is usually approximately the same as the gain of the whole stage, and in the case that it is large, this capacitance term dominates. For previous MiniCan preamps, the input capacitance is typically about 55 pF.

In the feedback preamp shown in Fig. 13, the preamp functions similarly to a non-inverting op-amp amplifier, but here the JFET source terminal acts as the equivalent to the inverting input. Because of this, a voltage follower effect is observed between the gate and the source voltages. The source voltage follows the voltage of the input which is the gate voltage. The gate to source capacitance C_{gs} is one of the largest capacitances of the whole system. (For low-noise JFET's is is usually 10 to 15 pF and the gate to drain capacitance is just 2-4 pF).

A great result of this design is that the source voltage "tracks" the gate voltage. Then it is obvious that there is no AC difference between the two points, while at the same time there is a DC voltage difference. Since the transconductance function of an FET is to modulate the drain to source current in a linear relationship to the gate to source voltage, we can see another interesting feature. The drain to source current is

approximately constant and thus the JFET drain terminal is roughly a virtual ground for AC signals. This results in a unity effective gate to drain gain AC voltage. The input capacitance is now estimated by

$$C_{input} = A_{V,gs} \cdot C_{gs} + A_{V,gd} \cdot C_{gd} = 0 \cdot C_{gs} + 1 \cdot C_{gd} = C_{gd} \tag{3.4}$$

The net result is a large reduction of the input capacitance, by roughly a factor of 10. In the case of small low-noise hydrophones, this can enable the use of much smaller piezoelectric source capacitances without a large signal loss caused by the preamplifier input capacitance.

6. Input Protection Diodes

The first stage of the amplifier consists of a high value gate resistance R_g and a low noise n-channel JFET with an input protective arrangement of four diodes configured in an asymmetric way. The resistor R_g is a necessity since it maintains the gate DC bias voltage at ground potential. It is large enough to satisfy the necessity for a high input preamplifier impedance.

The diodes connected to the input of the preamp are necessary to protect the JFET gate from damaging voltage levels generated by the piezoceramic. The gate to source junction of the JFET is essentially a PN junction diode. It can tolerate only a few mA of current in the forward direction at a silicon diode drop of 0.6 – 0.8 V, and 10's of volts of reverse bias voltage before destructive reverse breakdown occurs. Even a small piece of PZT ceramic can generate 100's of volts and many milliamperes of current when subjected to a modest mechanical impact.

A group of three series-connected diodes is connected between the gate and ground and has a zero DC bias voltage. This diode triplet protects the JFET gate from extreme negative input voltages. The dynamic impedance of these diodes should be at least two orders of magnitude larger than source impedance which can be in excess of 10 MΩ. When forward biased by as much as 200 mV or more by the AC input signal, the impedance of a single silicon diode may not be negligibly high. Thus, the purpose of the series connected diode triplet is to cut the forward bias voltage of each by a factor of 3 and increase the dynamic impedance of the diode triplet by 1 to 2 orders of magnitude compared to the impedance of one.

The single diode connected between the JFET gate and the two source resistors protects the gate from extreme positive input voltages. It is reversed biased by a DC voltage that is 60% to 80% of the source voltage. If the reverse bias voltage were 100% of the source voltage, the diode would fail to protect the JFET in some cases. With the reverse bias, the dynamic impedance of the diode is extremely high for input voltages up to the positive clipping level of the preamp.

The diodes that were selected for use in the preamplifier were new models demonstrating lower capacitance, medium forward conductance, and low reverse leakage. The medium forward conductance level results in a smaller exponential factor of their current to voltage curve (from the manufacturer sheet). Thus, they exhibit a larger dynamic resistance at 100 to 200 mV of forward bias than would a high conductance model. These diodes are packaged in pairs in surface mount packages, so only two components are required for the four diodes shown in the schematic.

7. Feedback Stability

When initial testing of the feedback preamp was performed by Hofler and Alvarado, the design was that of Fig. 13 except C_f and C_c were absent and $R_o = R_{e2} = 0$. The preamp was stable for output load capacitances up to roughly 200 pF, but oscillated at several hundred kHz for larger capacitive loads, rendering it useless for hydrophone use. The load capacitances used as a reference in the amplifier research were 2 nF, 4.7 nF and 10 nF that correspond to hydrophone cable of lengths 12 m, 27 m and 58 m, taking 52 pF/ft as the distributed capacitance.

Hofler and Alvarado discovered that by adding the frequency compensation component C_c in the range of several nF, the preamplifier was stable for all reference load capacitors. However, it was not understood until this thesis that the 2nd stage was not able to provide the current necessary to drive C_c for large signals above 5 kHz. A more normal situation would have had $C_c < 500$ pF, but this was not stable.

The purpose of capacitor C_c is to reduce the gain of the 2nd stage at very high frequencies, but this was not happening with low values of C_c because the impedances of C_e and C_c were tracking each other at high frequencies. The key to the problem was to introduce a small value resistive component R_{e2} in series with C_e to limit minimum value

of the emitter impedance at high frequencies. Then, a value of C_c in the range of a hundred pF was successful in stabilizing the amplifier, although the high frequency performance at this point was not ideal.

The initial attempts to solve the instability problem for this project were unsuccessful. Ultimately, much of the successful work in stabilizing the amplifier involved computer analysis of the circuit with SPICE software. The technique used requires a little explanation.

The occurrence of instability is associated with the open and closed loop gain of an amplifier.[24] The gain with negative feedback is

$$G = \frac{A}{1 + AB} \tag{3.5}$$

where A is the open loop gain without the presence of the feedback branch and the product AB is the closed loop gain.

Nevertheless, it can be shown that the open loop arrangement for amplifiers usually produces a phase shift in the signals (passing through them) with frequency, and that might cause a conversion of the negative feedback arrangement to a positive one. In every stage there is a phase shift due to the time lag inherited by the signal while it is amplified in the specific stage.

The result may be the oscillation of the circuit independently of the input signal. An indication of this can be determined by observing the reduction of the open loop gain above a certain mid-to-high frequency (breakover)[25]. As the frequency increases, the open loop gain falls up to the point that becomes unity. This should happen before the phase shift reaches the 180^o. Otherwise, instability is certain to occur.

When using computer analysis, it was not easy to determine the open loop gain response since the large DC current in the feedback loop became zero, which in turn altered the bias points of all of the stages. Instead, the gain and phase of the closed loop

[24] Neil Storey, pp. 138 and 140.

[25] Paul Scherz, *Practical* E*lectronics for Inventors*, McGraw Hill, 2000, p. 236.

response was determined numerically. The objective was to achieve a relatively flat closed loop gain response up to 500 kHz and a phase margin of 45° or better at unity closed loop gain, for the various values of load capacitance.

With trial and error, a satisfactory combination of values for C_c, C_f, and R_o was chosen, resulting in excellent performance.

8. Further Work to Achieve Low Noise Performance

After solving the stability issues with the preamplifier, measurements indicated that the equivalent input noise had increased by roughly 2 dB compared to the previous MiniCan preamps. Further work was performed to achieve the ultra-low-noise performance of the previous preamps.

A study of multi staged amplifiers[26] reveals that noise contributions of stages beyond the first should have virtually no effect on the Noise Figure (NF) of the system[27], especially when the first stage provides high gain. The feedback preamp discussed here does not follow the above assumption very well for the following reason: The 3rd stage emitter follower is driven by a moderately high source resistance (i.e. R_c) but carries a high bias current of several mA. This is a particularly bad combination for the noise performance of any BJT. Thus, while the noise performance of the 3rd stage should be of negligible importance, it is poor enough to be an issue.

The solution chosen was to optimize the component selection of the NPN transistor. This was difficult because the supplied datasheets failed to include noise performance data in this bad region of the parameter space. As a consequence, noise measurements were made in this region of the parameter space, as described below.

The section below presents the measured performance of the preamplifier.

B. PREAMP MEASUREMENTS

1. 3rd Stage Noise Minimization

When designing the preamplifier for the MCC, one of the primary goals was to achieve a very low equivalent input noise. The selection of a JFET as a first stage amplifier was made for its extremely high input impedance very low input noise current.

[26] C. D. Motchenbacher and F. C Fitchen, p. 37.

[27] NF is the dB expression of the ratio of input S/N to output S/N, which provides the total output noise power per unit bandwidth over the portion of output noise power caused by the source resistance.

Likewise, the particular JFET models were chosen for having unusually low equivalent input noise voltage. The criteria for the next two transistor stages, using a PNP and NPN BJT, were once again the noise specifications published by the manufacturer. Nevertheless, a series of measurements had to be made in order to ensure the best choice.

Among the two BJTs, the third stage transistor selection has been the most demanding. While the noise performance requirement of the third stage BJT is seemingly modest (given the high net voltage gain of the first two stages) its large bias current makes the component selection difficult. A typical bias current is roughly 4 mA, which is purposefully chosen this large in order to enable the preamp to drive large cable capacitances.

In order to observe the behavior of the candidate transistors for the third stage, the following arrangement was used:

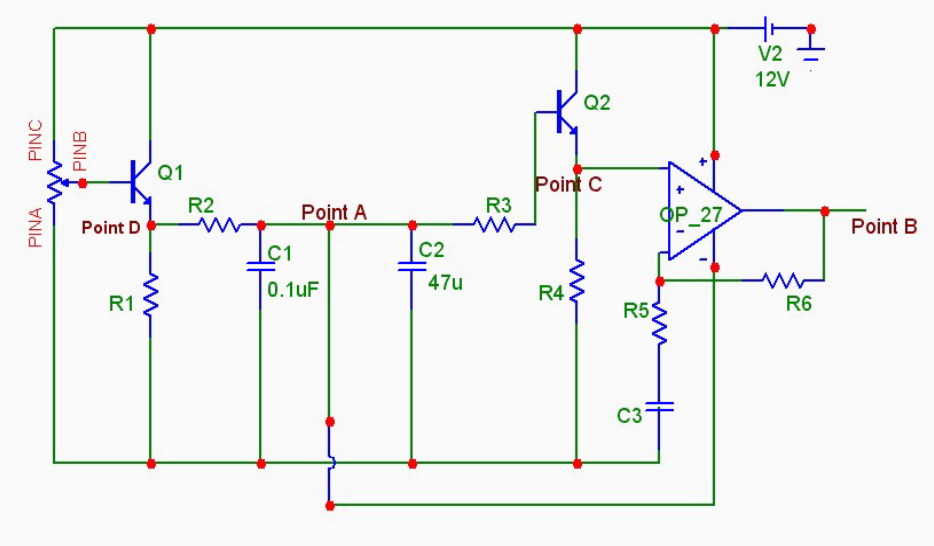

Figure 15. Protoboard Testing Arrangement

The op-amp chosen was the OP-27 model used in a non-inverting configuration which was utilized due to its low noise which is 3 $nV/Hz^{1/2}$ at 1 kHz. The resistors R_5 and R_6 give a gain of 11 or 20.8 dB, sufficient to increase the incoming noise signal of the transistor-under-test to a level well above the noise floor of the signal analyzer used. The "transistor-under-test" is named Q2 in the schematic, while another transistor Q1 has been used with the combination of a potentiometer as a voltage regulator. The circuit

contains small and large capacitors in order to reduce noise at high frequencies and the noise originated in the potentiometer. A Stanford Signal Analyzer SR785 processed the output signal and provided the following data.

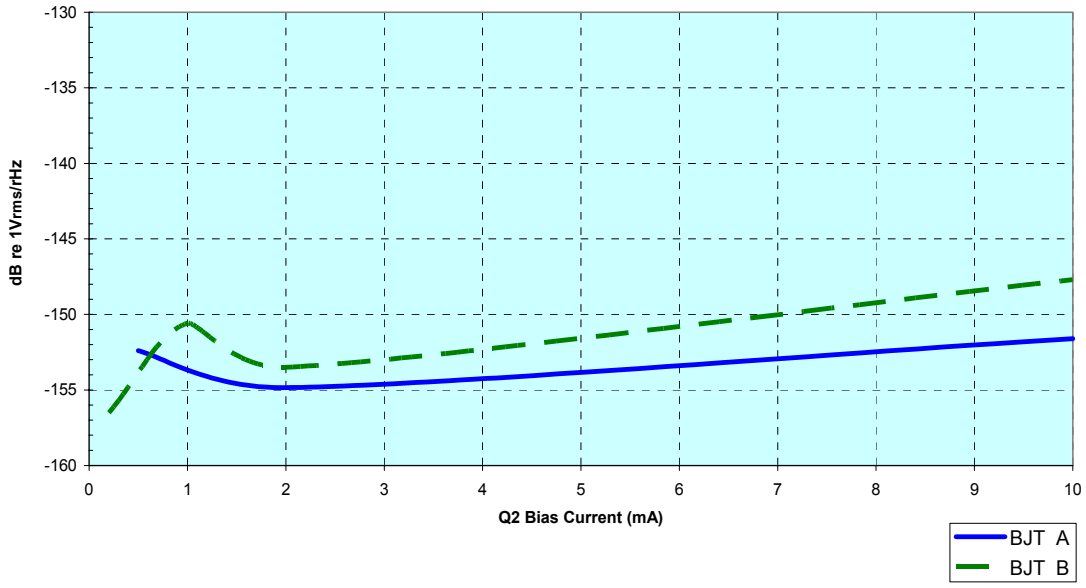

Figure 16. Receiving Results in dB re 1V/Hz$^{1/2}$ for Candidate NPN BJTs

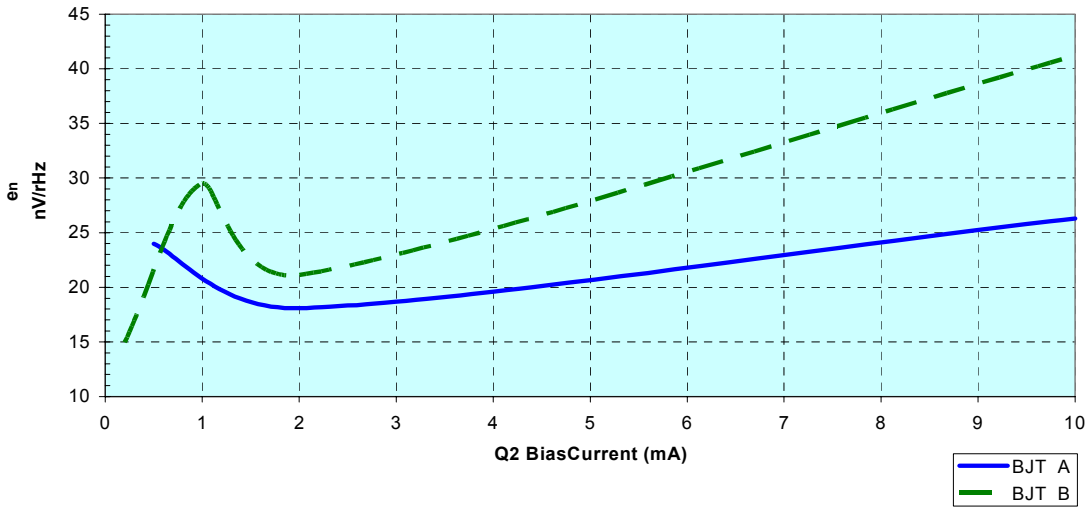

Figure 17. Receiving Results in nV/Hz$^{1/2}$ for Candidate BJTs. The Selected BJT A Has Obviously Better Noise Performance.

From the figures, it is observed that BJT "A" has better noise performance than the second one, and it was selected for the 3rd stage in the preamplifier.

The procedure for improving the preamplifier for MCC resulted in the construction of a few preamplifiers whose performance had been evaluated. Nevertheless, it is essential to refer to the specific preamplifiers used in the hydrophones MCC 2-1 and 2-2. The above preamplifiers are hereafter called preamp #13 and preamp #19 for convenience and they correspond to MCC 2-1 and MCC 2-2. Emphasis will be given to the results of the most advanced model which was preamp #19. Some data from much older preamps are also included in the next section for comparison purposes. Flex preamp #1 is one of the first 2-stage (no feedback) flexible preamps built, and preamp #11 is a 3-stage feedback preamp with only 2 input protection diodes.

2. Feedback Preamp Distortion

The feedback preamp handles large signals better with less distortion than the simple preamp of Fig. 14 for three reasons. First, the output current capability is much higher, which we will not attempt to show here. Second, the overall feedback increases the input voltage clipping level and reduces circuit nonlinearities because of the feedback process itself. Third, the novel input protection diodes also reduce the amount of distortion caused by the protection diodes. These last two effects are illustrated in Fig. 18 shown below.

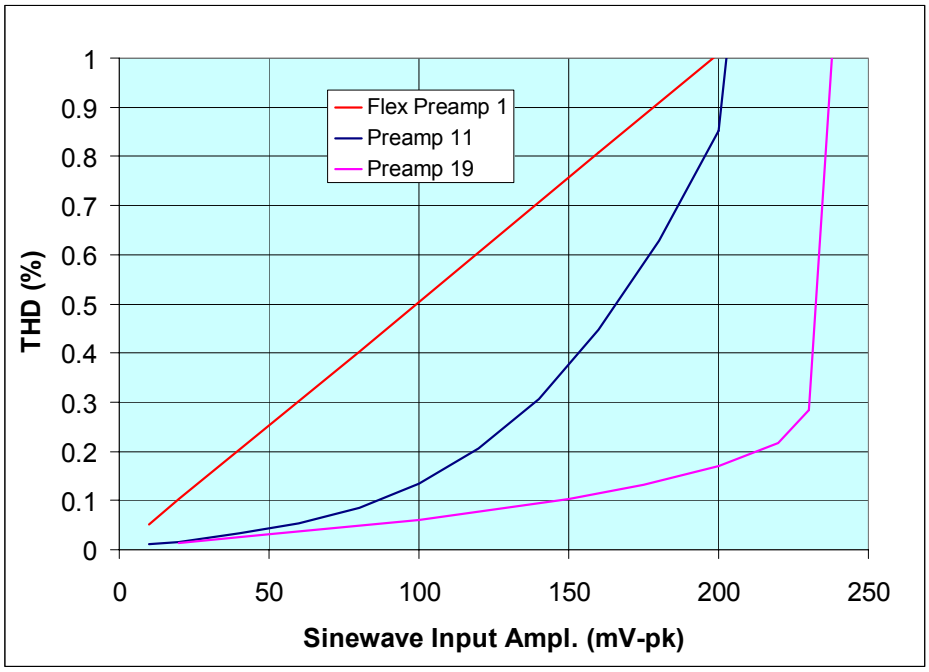

Figure 18. Preamp Distortions with 2-Diodes and No Feedback (#1), 2-Diodes Plus Feedback (#11), and 4-Diodes Plus Feedback (#19)

The test conditions for the measurement were: An input sinewave at 35 Hz and a signal source impedance of 220 pF.

3. Feedback Preamp Bias Voltages

The preamplifier's measurements are a sequential procedure which initially certifies the preamplifier's normal and desirable behavior, and then provides the values of gain and noise levels with respect to frequency.

The first measurements for the preamplifiers were the DC bias voltages with a shorted input. The preamp is fixed on a rigid board inside an aluminum box, hereafter called a tester.[28] The tester provides the necessary connectors for the power source (battery)[29], input and output signals and electrical shielding as well. The DC voltages measurement is executed in order to ensure that all the electrical components are soldered and connected properly. It is essential to short the input connection of the tester in order to avoid amplifying any stray AC signals.

[28] Miguel Alvarado, p. 21.

[29] Lead Acid PANASONIC battery 12 V, 1.3 Ah.

This was the first measurement performed on a newly constructed preamp because it allowed a quick determination of proper function. With the measured DC bias voltages and the resistance values, the DC bias currents could also be calculated. The actual measured values will not be listed here.

4. Feedback Preamp Clipping Levels

Thereafter, the stability and clipping levels had to be tested with a high precision digital oscilloscope Tektronix (TDS 420). The results for preamplifier #19 showed the input level where a lower order distortion was just initiated. When the frequency was fixed for various output coupling capacitances, the presented findings were recorded as follows.

Frequency	*Output capacitance*	*Maximum Input Voltage*
20 kHz	2.2 nF	209 mV_{pk}
20 kHz	4.7 nF	173 mV_{pk}
50 kHz	2.2 nF	224 mV_{pk}
50 kHz	4.7 nF	215 mV_{pk}

Table 7. Maximum Input Voltages during Clipping Measurements for Preamp #19

5. Feedback Preamp Bandwidth

An important factor in the preamplifier's operation is the available bandwidth, since this factor, in combination with the hydrophone's resonant frequencies defines the area of application in many cases. The Tektronix TDS 420 oscilloscope captured the measured values, and the points where the gain was reduced by -3 dB and -1dB were noted:

Point of interest	*Corresponding Frequency*
-1 dB	720 kHz
-3 dB	1.38 MHz

Table 8. Upper Bandwidth Limits for Preamplifier #19 Used in MCC 2-2

The point of -3 dB is of interest since it is the usual bandwidth limiting level. The –1 dB level is also shown for those who may have more stringent requirements. The lower frequency response behavior of preamp #19 is shown in the figure below. It is determined by the AC coupled emitter of the 2nd stage.

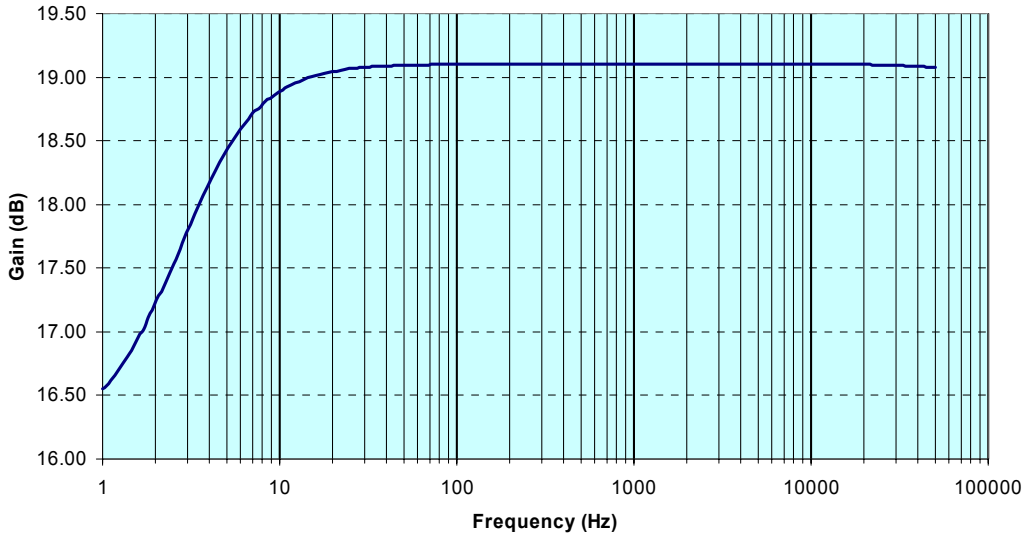

Figure 19. Preamplifier #19: Zero Source Impedance Frequency Response Gain Measurement

Subsequently, the gain and the preamplifier's input capacitance were determined applying the formula (3.3). The interested reader could gather more detailed information on the methods followed in the thesis by M. Alvarado.[30]

6. Feedback Preamp Input Capacitance

The preamplifier's effective capacitance can be found by measuring the preamp gain twice. First the gain is measured with a zero impedance signal source, then again with a low source capacitance in the range of 50 pF. Then the preamp's input capacitance is given by,

$$C_{input} = \frac{1 - A_R}{A_R} C_{source} \tag{3.6}$$

where $A_R < 1$ corresponds to the ratio of the high source impedance gain to the low (zero) source impedance gain, C_{source} is the signal source capacitance.

[30] Miguel Alvarado, pp. 21- 27.

7. Feedback Preamp Equivalent Input Noise Voltage

The preamplifiers' noise measurements refer to the noise generated by the electronic components with the input shorted. The noise voltage is measured at the output, but is then referred back to the input by dividing by the amplifier gain. The result is usually called an "equivalent" input noise level since it was not actually measured at the input. While the input noise voltage measurement does not include the input noise current, it has been found to be of negligible importance for these hydrophone designs.

The noise level was initially captured by the Stanford analyzer SR785 in units of dB re $V_{rms}/Hz^{1/2}$ as a function of frequency. Thereafter, it was converted to the Equivalent Input Noise Voltage (e_n).

The figures shown below indicated the noise performance of these preamplifiers. More specifically, both of them follow the usual low frequency or $1/f$ noise pattern, which then becomes almost constant over the upper part of the frequency span.

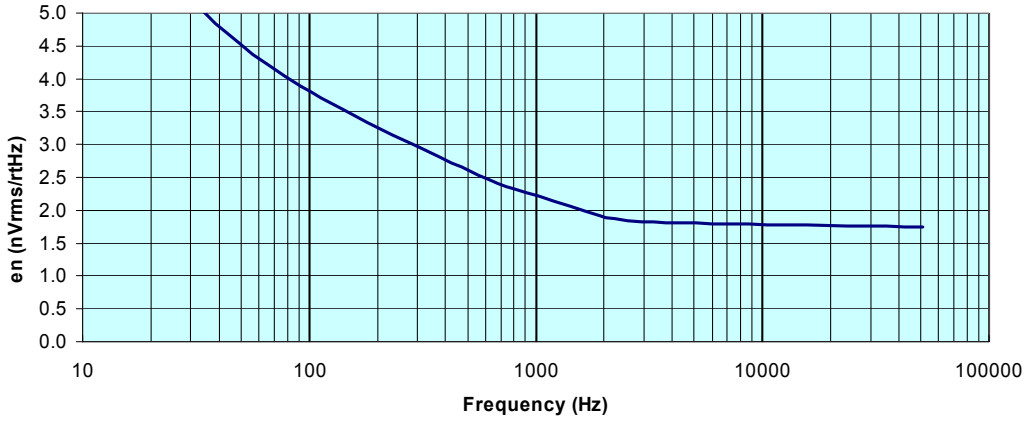

Figure 20. Equivalent Input Noise e_n in $nV_{rms}/Hz^{1/2}$ of Preamp #13

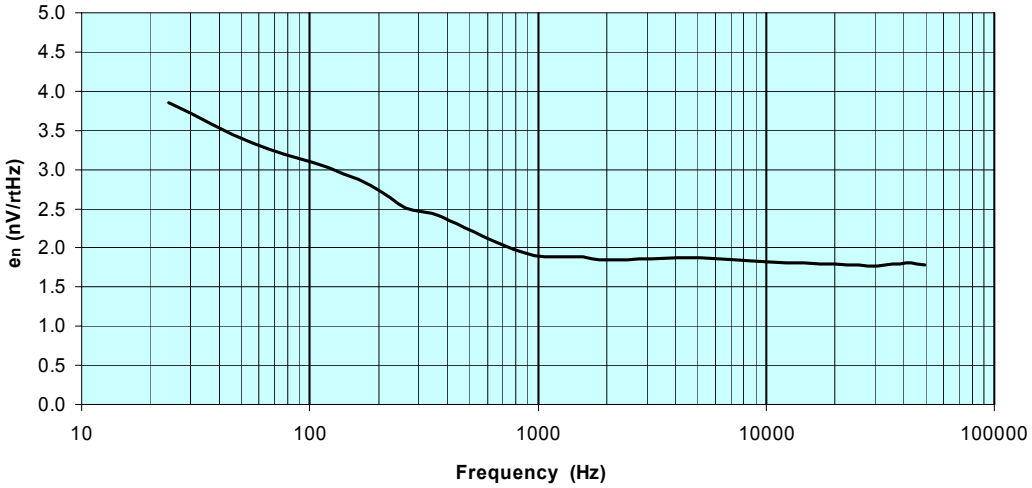

Figure 21. Equivalent Input Noise e_n in $nV_{rms}/Hz^{1/2}$ of Preamp #19

Both of these preamp exhibit excellent ultra-low-noise performance for an FET preamp. Note the low frequency noise performance of #19 is slightly better than #13. Preamp #19 was built exactly according to the schematic in Fig. 13, whereas preamp #13 was built with C_f and C_c absent and $R_{e2} = 0$. Unfortunately, this means that the maximum signal level capability of preamp #13 was very poor above 5 kHz.

8. Feedback Preamp Gain Tempco

A challenging question was posed concerning the temperature effects on the preamplifier's overall gain. The temperature coefficient of the gain was measured in a simple experiment. During the experiment, the temperature of the aluminum box tester, used as a platform for each preamplifier's self noise and gain measurements, was subjected to a temperature change from 20°C to 41°C. Simultaneously, the Stanford analyzer SR785 measured the gain frequency response of the preamplifier. The maximum percent change in the gain was 0.004%, corresponding to the maximum temperature change of $\delta T = 10\ ^{o}C$. Their ratio is 0.0004 ppm/°C. (ppm is parts per million) This tiny gain variation is comparable to the change expected in the resistance of high quality resistors.

THIS PAGE INTENTIONALLY LEFT BLANK

IV. MEASUREMENTS OF MINI CYLINDERCAN HYDROPHONES

A. SENSITIVITY MEASUREMENTS

The measurements performed on the constructed hydrophones consist of the following three categories:

- free field voltage sensitivity measurements
- vertical directivity pattern
- self noise pressure level measurements

Two Mini CylinderCan (MCC) hydrophones were tested in NPS facilities, and the calibration procedure includes the measurement of the pressure sensitivity in water and the measurement of the hydrophone's self noise in air. More specifically for the underwater calibration, the "side by side" method was followed using the Bruel & Kjaer 8103 hydrophone as a reference. The two hydrophones were placed next to each other separated by a distance of 6 in, a distance that is several times larger than the size of their diameters[31]. This separation is necessary in order to the effect of sound reflections that occur between the two hydrophones for the time period needed to do the measurements.

During the measurements, the correct separation distance from the sound source or "projector" is also required in order to achieve an incident plane wave on the hydrophones since the projector is spherical. This distance between the projector and the hydrophones is set at 28 in. which is considerably beyond the far field limit, and thus, the measurements are conducted in the far field region. The general limit for the far field is $r_{\min} \approx \frac{L^2}{4\lambda}$, where L is the longer transverse direction of the source and λ is the sound wavelength.[32] Therefore, the complexities of the acoustic near field are avoided.

The acoustical centers of the underwater devices were set at a depth of 42 in. in the NPS water tanks since this is the middle of the total depth.

---

[31] B&K 8103 outer diameter=0.374" and MCC outer diameter=0.375".

[32] L. Kinsler, A. Frey, A. Coppens and J. Sanders, *Fundamentals of Acoustics*, J. Wiley and Sons, Fourth edition, 2000, p. 191.

The pressure sensitivity of B&K 8103 reference hydrophone is reported as -211.7 dB re 1V/μPa from the manufacturer and the resulted sensitivity for both MCCs are presented in the graphs. It should be taken into consideration that an external preamplifier, a Stanford SR560 with a gain of +40 dB, has been used to amplify the reference hydrophone signal since it does not have an internal amplifying system and its sensitivity is low.

1. High Frequency Setting

The spherical ITC 1032 projector has been employed as projector for the range of frequencies above 1 kHz and the Stanford SR785 performed an impulse-FFT and frequency response ratio measurement on both hydrophones' signals.[33]

The resulting data from the signal analyzer is the response of the MCC relative to the response of the reference hydrophone. The frequency response of the reference hydrophone is assumed to be flat. This is true to a level of ±0.5 dB up to 50 kHz.

The omnidirectional spherical projector was driven by a single cycle sine pulse of 2.5 kHz frequency and a single square pulse of 25 kHz, 28 kHz, 60 kHz and 75 kHz, covering a signal analyzer frequency span from 0 Hz to 102.4 kHz.

The MCC sensitivity is calculated as the algebraic sum of the reference sensitivity and the amplitude ratio of the two signals measured by the FFT analysis. The reference sensitivity is the algebraic sum of the B&K 8103 sensitivity and the gain of the external amplifier. The sensitivity measured in this way is called an FFVS or Free Field Voltage Sensitivity.

2. Low Frequency Setting

The low frequency measurements were accomplished with a Dual Tri-Laminar Flexural Disk Projector (DTLFDP)[34]. The projector was driven by the Dynamic Signal Analyzer SR785 combined with a Techron power amplifier 5507 and a step up transformer turns ratio of 7.5. The drive signal was a Swept-sinewave with a settling time of about 200ms. The frequency response was measured from 100 Hz to 1 kHz. The

[33] The resonance frequency underwater for ITC 1032 is 33 kHz. Miguel Alvarado, *Construction and Testing of Low Noise Hydrophones,* Master's Thesis, Naval Postgraduate School, Monterey, California, 2003, p. 24.

[34] The flexural disk has a diameter of 3.5". The resonance frequency for DTLFDP is 1150 Hz in water. This projector has been constructed as a final project on the PH4454 course by NPS students.

distance between the hydrophones and the projector was the same as before. The two receiving hydrophones are now separated by less than 1 cm, while avoiding contact. The fact that the two hydrophones are so close to each other, makes it possible to measure the open circuit sensitivity (OCV) to pressure.

The OCV is not the same type of measurement as the FFVS. However, an OCV measurement made with mechanically rigid hydrophones at low frequencies where the wavelength is much larger than the hydrophone size, should be the same as an FFVS measurement. The resulting figures present the sensitivity as FFVS for the entire span of low to high frequencies, but the data below 1 kHz is actually OCV data.

3. Water Calibration Results

The calibration results exhibit the performance of each constructed hydrophone.

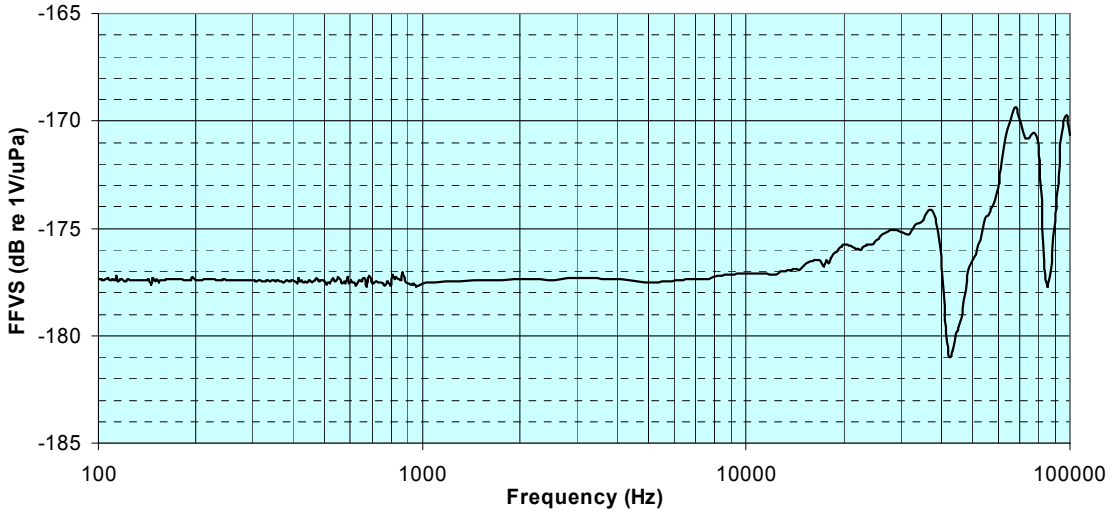

Figure 22. Total Free Voltage Sensitivity of Mini CylinderCan 2-1 Combining Two Different Sound Sources and Two Different Frequency Ranges

It is evident that MCC 2-1 achieves a high sensitivity compared to that of the B&K 8103 reference. The low frequency sensitivity for MCC 2-1 as shown in the above figure -177.4 dB re 1V/µPa, while for the frequencies above 10 kHz is -175.8 dB re 1V/µPa. Even after the gain of the internal preamp is factored out, the sensitivity of the MCC 2-1 is 14.8 dB higher than that of the B&K 8103.

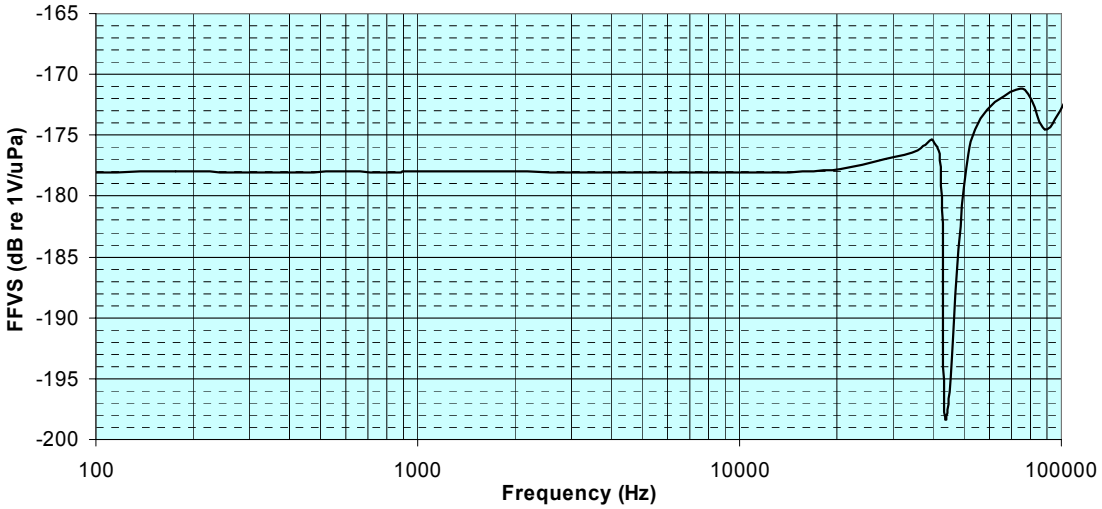

Figure 23. Total Free Voltage Sensitivity of Mini CylinderCan 2-2 Combining Two Different Sound Sources and Two Different Frequency Ranges

MCC 2-2 demonstrates a very nice sensitivity of -178.02 dB re 1V/μPa up to 20 kHz. Thereafter its sensitivity has an average value of 178.9 dB re 1V/μPa. The response of MCC 2-2 is similar to MCC 2-1, but achieving slightly higher sensitivity level. It is essential to have in mind that MCC 2-2 is operating with the improved preamplifier with all its beneficial features.

4. Vertical Directivity

It is valuable to the measure of the vertical directivity patterns of the hydrophones in a water tank, since these measurements indicate the frequency ranges where the omni-directionality of the hydrophone degrades. A special rigging structure was used to handle the hydrophone along with a rotational mechanism. The parts of the rigging were made of stainless steel due to its large modulus and corrosion resistance. In addition, they were given shapes, especially their end points, that would minimize any kind of signal reflection into the measurement area. The following figure presents the entire mechanism[35].

[35] R .J. Bobber, Underwater Electroacoustic Measurements, Naval Research Laboratory Publication, 1970, p. 118.

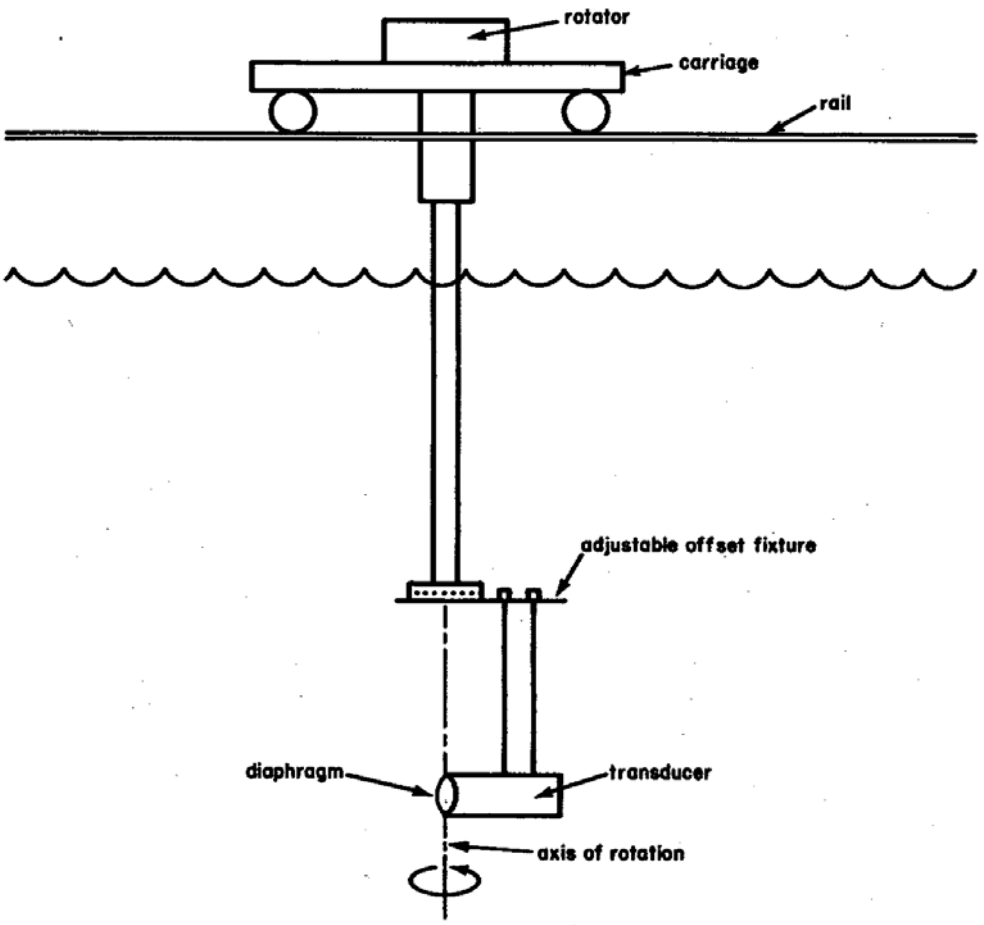

Figure 24. Rigid Rigging for Rotating the Hydrophone

The acoustic centre of the hydrophone is designed to be exactly at the center line of the main rod and the remainder of the structure was set as remote as possible from the transducer vibrating face. The dimensions of the horizontal bar are 4 ½ in. long and 3/32 in. thick with rounded edges. The vertical clamp attached to the hydrophone was 4 in. long.

Mini CylinderCan 2-1 proved to be roughly omni-directional for frequencies up to approximately 25 kHz and very omni-directional for frequencies up to 15 kHz. The figures below represent the vertical directivity patterns as recorded in the water tank at NPS. A linear arrangement of the reference hydrophone B&K 8103, the spherical projector ITC 1032 and the MCC hydrophone with separation of 28.5 in. was arranged

for the measurement. A rotator was used to rotate the hydrophone being tested with its longitudinal axis placed horizontally. The SR560 low noise preamplifier and the Stanford SR785 amplified the received signal from the B&K 8103 in coordination with a portable computer that analyzed the received data.

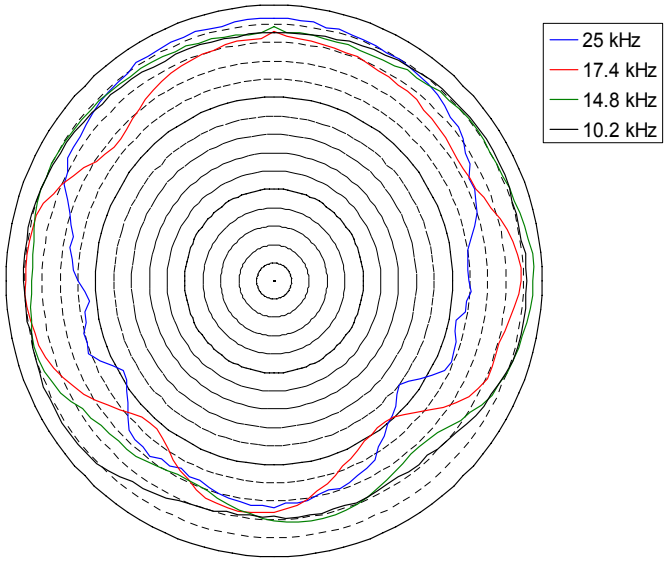

Figure 25. Vertical Directivity Pattern of MCC 2-1. Scale of 1 dB per Division

The figure shows that MCC remains roughly omni-directional for frequencies up to 25 kHz largely because of its small size.

B. SELF NOISE PRESSURE RESPONSE

The anechoic chamber was used as an appropriate place of minimal environmental noise in order to measure the self noise of MCC hydrophones. A low frequency mechanical filter was used in order to strongly attenuate room vibrations above 5 Hz. The SR560 low noise external amplifier amplified the noise signal while running on batteries to eliminate the 60 Hz harmonics in the measurements. The Stanford SR785 signal analyzer was used to measure the noise power spectral density of the amplified hydrophone signal. The results from the analyzer were a combination of two frequency regions, from 0-1.6 kHz and 0-51.2 kHz, providing the noise level in dB in reference to $1V_{rms}/Hz^{1/2}$. The noise voltage data is then divided by the low frequency pressure

sensitivity which yields the equivalent noise pressure or self-noise of the hydrophone. The following shows the results of the hydrophones in comparison with Wenz's and the Knudsen's sea state zero curves.[36]

The Knudsen sea state zero curve is a standard curve of the average ocean water ambient noise that exists under no-wind conditions (sea state zero).

Wenz's curve is the product of an effort to collect the lowest possible noise data taking into account the variability of the ambient noise in particular locations over a short period of time. The recorded noise originates from environmental (season of year, day or night) or biological changes. The noise sources of wind speed, amount of shipping, or other human activities are largely or entirely absent.

The above curves usually constitute the standard criteria for the noise performance of hydrophones. The measured data for MCCs are shown in the following figures.

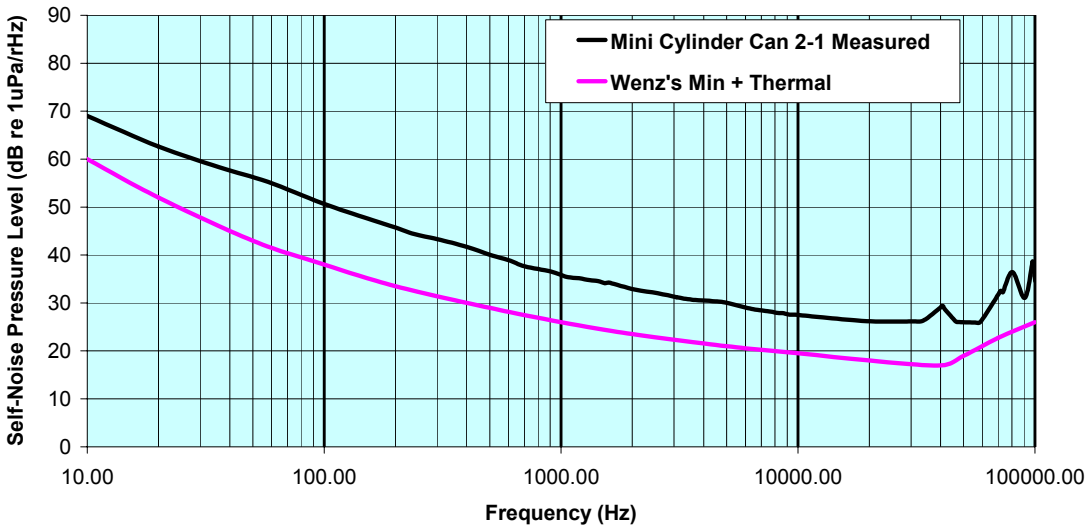

Figure 26. Self-Noise Pressure Level of MCC 2-1 in dB re 1 μPa/$\sqrt{Hz}$ Compared to Wenz's Minimum Plus Thermal Noise

[36] R. J. Urick, *Principles of Underwater Sound*, Peninsula Publications, Third edition, 1983, p. 215 and D. Ross, *Mechanics of Underwater Noise*, Peninsula Publications, 1987, p. 69.

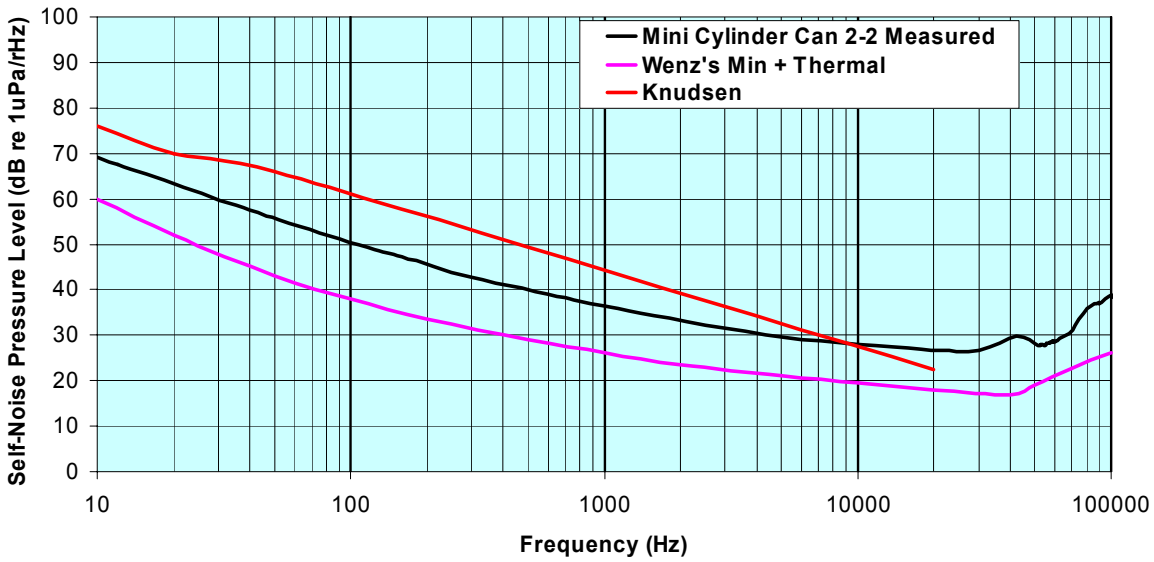

Figure 27. Self-Noise Pressure Level of MCC 2-2 in dB re 1 μPa/$\sqrt{Hz}$ Compared to Wenz's Minimum Plus Thermal Noise and the Knudsen Sea State Zero Noise

The results show the expected noise characteristics of both MCCs. The noise levels are above the Wenz's minimum noise level but are relatively close to it, at about 10 dB up to 10 kHz, and then approach it at approximately 8-9 dB for higher frequencies. The noise behavior of the MCC hydrophones is nearly as good to commercial hydrophones such as B&K 8106 in spite of a size that is roughly a factor of 4 smaller. At this point also, the theoretical calculations had predicted a total noise of 26.27 dB re1 μPa/ $Hz^{1/2}$ for MCC 2-1 and the total noise measured is 26.8 dB re1 μPa/ $Hz^{1/2}$, while for MCC 2-2, it was measured 27.6 dB re1 μPa/ $Hz^{1/2}$. Thus, there is a difference of -0.53 dB re1 μPa/ $Hz^{1/2}$ and -1.33 dB re1 μPa/ $Hz^{1/2}$ relative to the theory.

V. DISCUSSION

During the conception and construction procedure of the Mini CylinderCans, it became clear that, on the one hand, the entire process was interesting, but on the other, it was demanding and required thoroughness and detail. Starting from the point of defining the right dimensions for every part of the device, several needs had to be satisfied.

A major concern was the relocation of the resonance frequencies of previous models to higher regions. The thickness and shape of the lid was modified in order to increase the flexural stiffness in this part. As described in Chapter II, the increased thickness of the lid also made it more massive. Thus, the flexural resonance should move towards higher frequencies.

The rest of the alterations of the MCC parts, such as the change of material for the cable fitting part from stainless steel to aluminum 6061-T6 or the reduction of thickness for the bottom part of the tube, was also an effort to increase the resonance frequency of the tube that holds the preamplifier.

A mold for encapsulating both MCCs did not exist. The method of application of urethane to the outside, created regions of non-uniform urethane thickness with possible effects on the pressure sensitivity for the MCC 2-1 hydrophone. In the case of MCC 2-2, a partial coverage with polyurethane was decided in order to mitigate the possibility of bubbles existing in the protecting layer. A small amount of urethane was placed around the main body and the fitting to ensure water tightness.

Furthermore, small dimensions of the MCC hydrophones are desirable since hydrophones should operate in an omnidirectional way, avoiding at the same time any diffraction effects.[37]

The theoretical capacitance for the used stack of PZTs was calculated to be 150.1 pF while the measured ones were found to be 157.8 pF for MCC 2-1 and 157.4 pF for MCC 2-2, proving that there is a good agreement with manufacturer's data.

[37] For hydrophones of dimensions larger than the half sound wavelength, usually diffraction effects occur. Stansfield, p. 279.

The noise of the preamplifier remained at competing levels with respect to commercial hydrophones that are at least 4 times as large, but still approximately 10 dB more than that achieved with Mini Can 6. The noise of the final preamp (#19) was measured to be less than 3 $nV_{rms}/Hz^{1/2}$ for 100 Hz to 1 kHz and approximately constant at 1.8 $nV_{rms}/Hz^{1/2}$ above 1 kHz. This noise level is very satisfactory in spite of the PZT's capacitance decrease stated earlier, and it is still closer to the Mini Can 6 performance than most other commercial models.

The feedback feature was an important feature in the preamp's design, since it assisted in stabilizing the gain with respect to temperature change and reduced the distortion level to 0.2 % for 200 mV_{pk} input signal. The surprising and beneficiary results in the preamplifier's performance were:

- the decrease of the effective input capacitance for the preamplifier,
- the increase of the input voltage signal levels without distortion
- the increase of the output current without distortion

Both MCC hydrophones have high sensitivities that agree well with theoretical prediction with less than 1 dB deviation. Their frequency response is flat up to 40 kHz and 42 kHz for the MCC 2-1 and 2-2 respectively.

The self noise of the hydrophones was satisfactory although it remains above Wenz's minimum by approximately 10 dB since this was expected from the starting point of their design. These noise levels still represent excellent noise performance since ocean environment noise levels are seldom as low as Wenz's minimum. The positive point is that they remain comparable to commercial hydrophones that are much larger and more expensive. The noise performances of both were better than the Knudsen's sea state zero curve.

The polar vertical directivity patterns indicated omni directionality up to frequencies of approximately 15 kHz with a 2 dB variation in the pattern. The directivity was moderately omni-directional (5 dB variation) at 25 kHz. Further deviations from the omni pattern could be subject to more analytical measurements.

VI. CONCLUSIONS

This thesis has discussed designing, building, and testing a simple, low cost hydrophone. The preamplifiers and hydrophones constructed succeeded in displaying flat frequency responses up to higher frequencies than earlier models, a relatively low noise performance and high pressure sensitivity. The fact that their cost remains low and their construction steps not too difficult, grants them the potential of competing and perhaps beating several commercial hydrophones.

A further investigation examining the inner design of the main body, such as the size of the step on which the PZT is mounted, or even a change in the lid's shape, could produce interesting results and better performance.

The polar vertical directivity patterns have not been as satisfactory as desired, in spite the small dimensions of the hydrophone. It is possible that there remain problems with the underwater calibration procedure. The explanation and the resolution of the upper limit for omnidirectionality of the MCC could be a subject of further analysis and investigation.

THIS PAGE INTENTIONALLY LEFT BLANK

LIST OF REFERENCES

1 Anan'eva, Alevtina Aleksandrova, *Ceramic Acoustic Detectors,* translated from Russian, Consultants Bureau, New York, 1965.

2. American Piezo Ceramics International Ltd, *Physical and Piezoelectric Properties of APCI Materials*. Available [online] at http://www.americanpiezo.com/materials/apc_properties.html, accessed 29 October 2003.

3. Bobber, J. Robert, *Underwater Electroacoustics Measurements,* Naval Research Laboratory Underwater Sound Reference Division, Orlando, Florida, 1970.

4. Bruel & Kjaer Sound and Vibration Measurement Inc., hydrophones brochure, Available [online] at: http://www.bk.dk, accesed 21 August 2003.

5. Hill, Winfield, Horowitz Paul, *The Art of Electronics,* First Edition, Cambridge University Press, 1983.

6. Lawrence Kinsler E., Frey, Austin R., Coppens, Alan B. and Sanders, James V., *Fundamentals of Acoustics,* Fourth Edition, John Wiley & Sons, 2000.

7. Storey, Neil, *Electronics A Systems Approach,* Second Edition, Addison-Wesley Longman Ltd, 1998.

8. Urick, Robert J., *Principles of Underwater Sound,* Third Edition, Peninsula Publishing Los Altos California, 1996.

9. Wenz, Gordon M., *Acoustic Ambient Noise in the Ocean: Spectra and Sources,* J. Acoust. Soc. Am. 34, 1962.

10. Wilson, Oscar Bryan, *Introduction to Theory and Design of Sonar Transducers,* Peninsula Publishing Los Altos California, 1988.

11. Stansfield, D., *Underwater Electroacoustic Transducers*, Bath University Press and Institute of Acoustics, 1991.

12. C. D Motchenbacher and F. C. Fitchen, *Low Noise Electronic Design*, Wiley Interscience, 1972.

THIS PAGE INTENTIONALLY LEFT BLANK

INITIAL DISTRIBUTION LIST

1. Defense Technical Information Center
   Ft. Belvoir, Virginia

2. Dudley Knox Library
   Naval Postgraduate School
   Monterey, California

3. Professor Thomas Hofler, Code PH/HF
   Department of Physics
   Monterey, California

4. Professor Bruce Denardo, Code PH/DE
   Department of Physics
   Monterey, California

5. Chairman, Physics Department
   Naval Postgraduate School
   Monterey, California

6. Hellenic Navy General Staff
   Personnel and Training (B) Branch
   Holargos, Greece

7. LT Konstantinos Bakas
   Vironas - Athens, Greece